Tuo et al. *Zool. Res.* 2026, 47(3): 706−726
https://doi.org/10.24272/j.issn.2095-8137.2025.567
https://cstr.cn/32248.14.zr.2025.567

ZR | Zoological Research

Review Open Access

Animal models for calcium oxalate kidney stone research

Xingyuan Tuo[1,#], Chao Cheng[1,#], Jun Wen[1], Liyuan Xiang[1], Shijian Feng[1], Kunjie Wang[1,*], Xi Jin[1,*]

[1] *Department of Urology*, *Institute of Urology (Laboratory of Reconstructive Urology)*, *West China Hospital*, *Sichuan University*, *Chengdu*, *Sichuan* 610041 *China*

ABSTRACT

Calcium oxalate (CaOx) stones are the most prevalent form of nephrolithiasis and are characterized by a substantial risk of recurrence. Their pathogenesis arises through distinct etiological pathways, including idiopathic metabolic susceptibility, monogenic disorders such as primary hyperoxaluria, enteric hyperoxaluria, and toxicant-associated injury, and is shaped by two primary papillary mechanisms: Randall's plaque formation and ductal plugging. A central translational limitation is that most experimental systems, particularly chemically induced rodent models, rely on acute hyperoxaluria. These models capture crystal nucleation, aggregation, and deposition but do not adequately recapitulate the decades-long natural history of idiopathic CaOx stone disease in humans or the gradual formation of Randall's plaques. This review systematically evaluates CaOx stone models in mice, rats, *Drosophila*, pigs, dogs, and cats, with an emphasis on induction methods, analytical endpoints, strengths, limitations, and applications in mechanistic research, drug discovery, and surgical instrument evaluation. Particular attention is given to plaque-related models such as *Abcc6* deficiency, etiologically aligned models of primary and enteric hyperoxaluria, and naturally occurring disease in companion animals. Finally, this review proposes a stepwise framework for selecting CaOx stone animal models according to research objectives, etiological relevances, pathological mechanisms, and translational applications.

Keywords: Animal model; Kidney stone; Calcium oxalate; Gene knockout; Randall's plaque

INTRODUCTION

Nephrolithiasis is a major urological disorder with an increasing global burden (GBD 2021 Urolithiasis Collaborators, 2024; Howles & Thakker, 2020; Peerapen & Thongboonkerd, 2023). Calcium oxalate (CaOx) stones constitute the predominant form of kidney stone disease and arise through complex etiological pathways, including idiopathic metabolic susceptibility shaped by genetic background, diet, and urinary microenvironment; monogenic disorders such as primary hyperoxaluria; enteric hyperoxaluria secondary to malabsorption; and toxicant-associated injury, including ethylene glycol (EG) exposure (Alexander et al., 2022; Khan et al., 2021; Singh et al., 2022). Across these contexts, pathological CaOx crystal accumulation represents a central event in stone formation and reflects disruption of the equilibrium between lithogenic factors and endogenous inhibitors of crystallization (Wang et al., 2021).

Two papillary processes have been proposed as major initiating mechanisms in kidney stone formation: Randall's plaques and Randall's plugs (Evan et al., 2007; Khan et al., 2012, 2021; Randall, 1936; Singh et al., 2022). The plaque pathway can evolve over decades and is poorly predicted by short-term urine chemistry measurements (Daudon et al., 2015; Kok et al., 2017; Worcester & Coe, 2010), whereas stones associated with tubular plugging are more often accompanied by pronounced biochemical abnormalities (Daudon et al., 2015; Worcester & Coe, 2010). Recent clinical and pathological studies have indicated that Randall's plaques are present in most individuals who form calcium-based kidney stones (Daudon et al., 2015; Evan et al., 2007; Kok et al., 2017; Worcester & Coe, 2010). These lesions consist of calcium phosphate (CaP) deposits in the renal interstitium that can extend through the papillary urothelium, creating exposed surfaces for CaOx crystal adhesion, overgrowth, and eventual stone formation (Daudon et al., 2015; Evan et al., 2007; Khan et al., 2012, 2021; Randall, 1936). A major obstacle in experimental stone research is that most animal models produce rapidly formed tubular crystal deposits within the kidney, often at the corticomedullary junction, rather than papillary-associated stones that develop within the renal pelvis (Khan, 2010; Khan & Glenton, 2010; Liu et al., 2025; Okada et al., 2007; Tzou et al., 2016). This mismatch limits the capacity of such models to reproduce idiopathic human CaOx stone disease (Daudon et al., 2015; Evan et al., 2007; Khan et al., 2021). Therefore, selection of an appropriate animal model requires explicit alignment among human etiology, target pathophysiology, and research questions. These

Received: 28 February 2026; Accepted: 16 March 2026; Online: 17 March 2026

Foundation items: This work was supported by the Sichuan Science and Technology Program (2024NSFSC1495), Sichuan Science and Technology Program (2024ZYD0053), and Program of Sichuan University (2023SCUH0054)

[#]Authors contributed equally to this work

*Corresponding authors, E-mail: wangkj@scu.edu.cn; jinxi@wchscu.cn

relationships are summarized in Figure 1.

This review provides a cross-species evaluation of CaOx stone models, with emphasis on model development, detection endpoints, and failure modes. It further maps available models to specific human etiologies and experimental objectives, including mechanistic investigation, high-throughput screening, safety assessment, and surgical instrument evaluation, and proposes practical recommendations for model optimization and reporting. Establishing a stepwise CaOx stone model selection framework may improve experimental efficiency and strengthen the translational relevance of preclinical findings. The proposed framework is summarized in Figure 2.

MOUSE MODELS

Comparisons of mouse and human kidney anatomy

Rodent nephrons differ from human nephrons in several structural and segmental features that are relevant to CaOx stone modeling. In rodents, the medullary thick ascending limb (M-TAL) shows a relatively uniform length across nephron populations, independent of the length of the loop of Henle (Bankir et al., 2020), whereas the cortical thick ascending limb (C-TAL) varies depending on the position of the glomerulus within the renal cortex (Bankir et al., 2020). Transcriptomic analyses further indicate that Umod expression is higher in the C-TAL than in the M-TAL in both mouse and human kidneys (Tokonami et al., 2018).

Mice also have a markedly smaller nephron count than humans, with approximately 9 000–18 000 nephrons per kidney compared with approximately 0.9–1.0 million in humans, and possess a single-papillary kidney architecture (Huang et al., 2021; Khan, 2010). Despite these differences, the microscopic organization of the mouse kidney, including glomerular structures, tubular compartments, and renal vascular network, broadly resembles that of the human kidney (Tzou et al., 2016). The mouse and human genomes are also comparable in scale, each containing approximately 3.1 billion base pairs, with an average sequence identity of about 85%, exceeding 95% in certain regions (Tzou et al., 2016). Adult mice typically weigh 25–35 g, corresponding to approximately 1/2 500 of average human body weight (Meneton et al., 2000). Each mouse kidney accounts for around 0.8% of total body weight, a higher relative proportion than that observed in humans (0.2%), indicating a greater kidney-to-body-weight ratio in mice (Meneton et al., 2000).

Hyperoxaluria models

Most mouse models of CaOx nephrolithiasis employ hyperoxaluria as the principal lithogenic stimulus, with systemic oxalate burden increased through exogenous substrates that enter distinct metabolic routes (Ermer et al., 2023; Khan & Glenton, 2010; Tzou et al., 2016). EG permits prolonged exposure but produces off-target toxicity and often requires additional lithogenic conditions, such as hypercalciuria, to generate substantial renal crystallization (Ermer et al., 2023; Mo et al., 2007; Wesson et al., 2003). Glyoxylate, a direct oxalate precursor, induces rapid and reproducible crystal deposition, although the effective dose range is constrained by lethality (Khan & Glenton, 2010; Liu et al., 2025; Okada et al., 2007; Yang et al., 2025). Hydroxy-L-proline (HLP) increases endogenous glyoxylate and oxalate

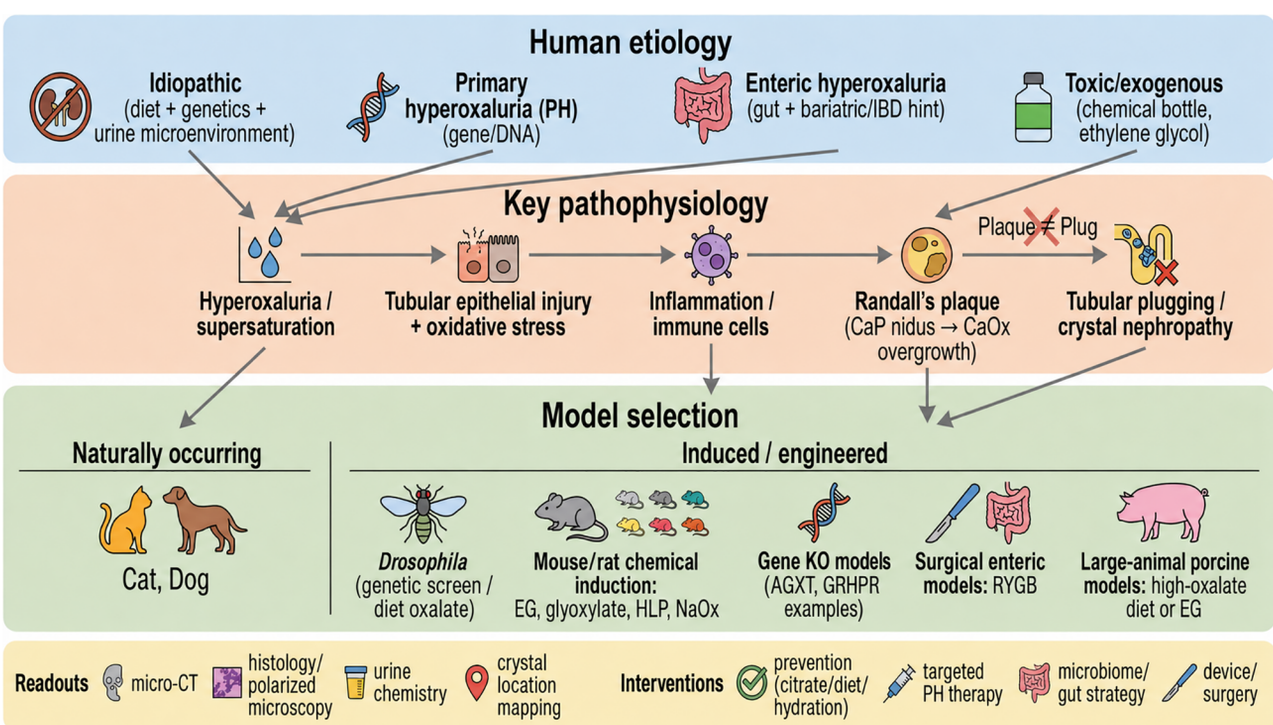

Figure 1 Calcium oxalate kidney stones: Human etiology, key pathophysiology, and model selection

Major clinical etiologies, including idiopathic metabolic risk, primary or monogenic hyperoxaluria, enteric hyperoxaluria, and toxic or exogenous exposure, converge on urinary supersaturation, epithelial injury, oxidative stress, and inflammation. Two papillary routes are highlighted: Randall's plaque-associated CaP nidus formation with CaOx overgrowth and tubular plugging/crystal nephropathy. The lower panel maps research questions to model selection, including naturally occurring companion animal disease, induced rodent hyperoxaluria models, genetic models such as primary hyperoxaluria models, surgical enteric hyperoxaluria models, and large-animal porcine models. Common readouts and intervention categories are indicated.

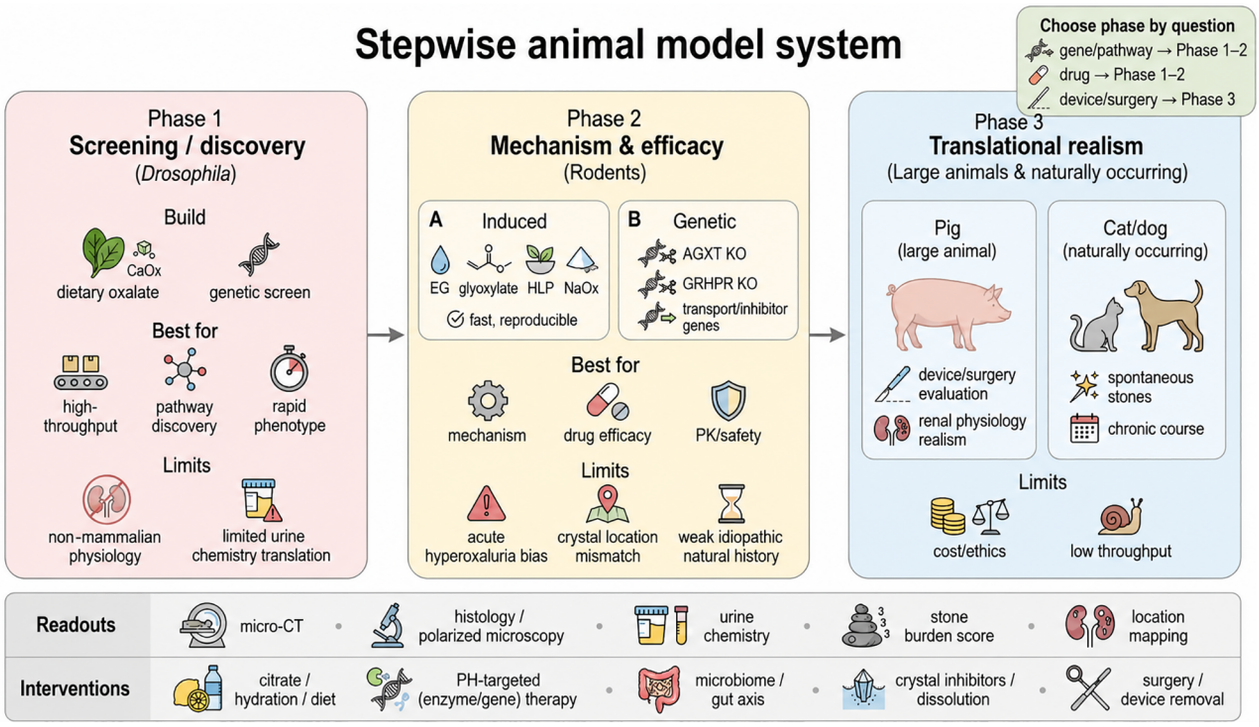

Figure 2 Stepwise animal model system for CaOx stone research

Phase 1 (screening or discovery): High-throughput *Drosophila* models for rapid pathway discovery and candidate compound screening. Phase 2 (mechanism and efficacy): Rodent models, including chemically induced and genetic etiological models, for mechanistic validation, pharmacological evaluation, and safety assessment. Phase 3 (translational realism): Large-animal porcine models and naturally occurring companion animal models, including cats and dogs, for chronic physiology, device and surgical evaluation, and clinically relevant stone management. Typical strengths, limitations, and preferred readouts for each phase are summarized.

metabolic flux and can be incorporated into the diet, but its utility is limited by systemic and renal toxicity (Knight et al., 2006; Knight & Holmes, 2005). Sodium oxalate (NaOx) provides oxalate directly and is particularly suitable for studying intestinal metabolism and microbiome effects (An et al., 2025; Hanstock et al., 2024; Khan & Glenton, 2010). Inducer selection should therefore be guided by the experimental objective, with careful consideration of induction kinetics, pathological fidelity, reproducibility, and toxicity (Khan & Glenton, 2010; Tzou et al., 2016).

NaOx: Hyperoxaluria is a primary driver of CaOx crystallization and stone formation (An et al., 2025). Dietary NaOx offers a direct strategy for increasing intestinal and urinary oxalate exposure. In C57BL/6 mice, two weeks of feeding with a diet supplemented with 1.5% NaOx induced hyperoxaluria in the urinary and intestinal compartments and produced stable renal CaOx crystal deposition (Hanstock et al., 2024).

EG: EG is metabolized primarily in the liver through sequential oxidation. Alcohol dehydrogenase first converts EG to glycolaldehyde, which is further oxidized by aldehyde dehydrogenase to glycolic acid and then metabolized through glyoxylic acid to oxalic acid (Ermer et al., 2023).Although EG induces hyperoxaluria in mice, this condition alone generally produces little or no renal CaOx crystal deposition (Mo et al., 2007; Wesson et al., 2003), with robust CaOx stone formation dependent on concomitant hypercalciuria (Khan & Glenton, 2010).

Glyoxylate: Glyoxylate is a proximal precursor of oxalate biosynthesis and has been successfully employed as an exogenous lithogenic agent to establish mouse models of hyperoxaluria and CaOx nephrolithiasis (Khan & Glenton, 2010; Liu et al., 2025; Okada et al., 2007; Yang et al., 2025). This model is commonly generated by intraperitoneal injection, with the dose and administration schedule strongly influencing model efficiency and animal survival. Okada et al. (2007) reported that doses of at least 60 mg/kg/day induced crystal formation by the third day of administration, whereas 80 mg/kg/day produced the most stable and reproducible phenotype, with higher exposure increasing mortality. Continuous administration of 100 mg/kg/day for 5–7 days has also been shown to induce hyperoxaluria and promote CaOx monohydrate (COM) crystal deposition at the corticomedullary junction in mice (Liu et al., 2025). The genetic background of mice also affects glyoxylate tolerance (Liu et al., 2025). Notably, high mortality rates have been reported in RXRα-deficient ($RXR\alpha^{-/-}$) mice treated with 80 mg/kg/day, with long-term survival requiring a dose reduction to 70 mg/kg/day (Liu et al., 2025). This suggests that glyoxylate-based model design should incorporate both the intended disease phenotype and strain-specific sensitivity to oxalate precursor loading.

HLP: HLP is a glyoxylate precursor that is metabolized within mitochondria of hepatocytes and proximal tubular epithelial cells, thereby increasing endogenous glyoxylate and oxalate production (Knight et al., 2006; Knight & Holmes, 2005). As a major collagen-derived amino acid, HLP is also present in ordinary dietary sources. Similar to EG and glyoxylate, HLP has been shown to induce hyperoxaluria in mice; however, a 5% hydroxyproline diet administered for 28 days failed to establish a complete renal calculus model (Khan & Glenton, 2010). Furthermore, despite effective induction of hyperoxaluria, severe systemic and renal toxicity caused death in all hypercalciuric male mice and marked weight loss

in normal mice, preventing completion of the experimental protocol (Khan & Glenton, 2010).

Gene knockout models

Primary hyperoxaluria: Genetic mouse models of primary hyperoxaluria (PH) provide a mechanistically defined platform for studying oxalate overproduction, renal calcium deposition, and CaOx stone formation. *Agxt* deficiency, which models PH type 1, causes hepatic oxalate overproduction, severe hyperoxaluria, and renal CaOx deposition, and has been used to evaluate substrate reduction, enzyme replacement, and liver-targeted gene therapy strategies (Salido et al., 2006). Models targeting the *Grhpr* gene, which represents PH type 2, develop hyperoxaluria or nephrocalcinosis, with hydroxyproline challenge further amplifying the phenotype and enabling assessment of pathway-specific interventions (Knight et al., 2012). Although primary hyperoxaluria models provide strong etiological fidelity for monogenic stone disease, they cannot replicate the multifactorial and slowly evolving natural history of idiopathic CaOx nephrolithiasis. Genetic models are therefore most informative when the research question centers on a well-defined pathogenic mechanism, such as primary hyperoxaluria, altered intestinal oxalate transport, or impaired urinary crystal inhibition, or when targeted interventions, including enzyme replacement and gene therapy, are being tested (Deguchi et al., 2024; Dong et al., 2022; Mo et al., 2004, 2007; Song et al., 2023; Taguchi et al., 2020; Wesson et al., 2003; Yamashita et al., 2020; Yuan et al., 2025; Zhu et al., 2019). Because different knockout techniques disrupt distinct stages of oxalate metabolism, epithelial transport, and crystal inhibition, the resulting phenotypes differ substantially, and no single genetic model captures the etiological diversity of human CaOx urolithiasis. Consequently, genetic models are often paired with dietary or chemical stimuli to accelerate crystal formation, reduce inter-animal variability, or model clinically plausible secondary triggers associated with idiopathic stone disease (Khan & Glenton, 2010; Tzou et al., 2016; Deguchi et al., 2024; Dong et al., 2022; Mo et al., 2004, 2007; Song et al., 2023; Taguchi et al., 2020; Wesson et al., 2003; Yamashita et al., 2020; Yuan et al., 2025; Zhu et al., 2019). Specific details are provided in Table 1.

Slc26a family: Sulfate transporter 1 (Sat1), encoded by *SLC26A1/Slc26a1*, is expressed on the basolateral membrane of proximal tubular cells and mediates sulfate and oxalate transport (Dawson et al., 2010). Sat1 deficiency disrupts renal oxalate handling and produces hyperoxaluria, with CaOx stone formation in renal tubules and the bladder (Dawson et al., 2010).

SLC26A6 is an apical anion exchanger in renal and intestinal epithelial cells that mediates Cl^--oxalate exchange and contributes to oxalate homeostasis (Dawson et al., 2010; Jiang et al., 2006). Slc26a6-deficient mice exhibit marked hyperoxaluria, elevated plasma oxalate levels, and increased susceptibility to CaOx urolithiasis, whereas dietary oxalate restriction significantly alleviates these symptoms, consistent with impaired intestinal oxalate secretion and increased net oxalate absorption in this model (Jiang et al., 2006).

Although SLC26A3 belongs to the oxalate exchanger family, it contributes to intestinal oxalate absorption rather than oxalate secretion, with SLC26A3 deficiency shown to reduce urinary oxalate excretion by approximately 70% (Cil et al., 2022; Freel et al., 2013). Based on this mechanism, small-molecule inhibition of SLC26A3 was tested as a therapeutic strategy in a dietary murine model of oxalate nephropathy and shown to reduce both hyperoxaluria and CaOx crystal deposition (Cil et al., 2022; Freel et al., 2013).

OPN and THP: OPN and THP are urinary macromolecules that regulate calcium crystallization and modulate CaOx crystal retention *in vivo* (Devuyst et al., 2005; Serafini-Cessi et al., 2003). OPN is a widely expressed phosphorylated glycoprotein, whereas THP is a kidney-specific glycoprotein and one of the most abundant proteins in urine (De Yoreo et al., 2006; Devuyst et al., 2017; Giachelli & Steitz, 2000; Nanamatsu et al., 2024). Functional studies support complementary protective roles for these proteins. Administration of 1% EG in drinking water induced substantial renal tubular CaOx deposition in OPN-knockout mice (Wesson et al., 2003), whereas combined EG and vitamin D administration markedly increased renal calcium crystal formation in THP-knockout mice (Mo et al., 2004). In high-calcium or high-oxalic acid environments, 10% of OPN-deficient mice and 14.3% of THP-deficient mice spontaneously formed crystals in the interstitium of renal papillae, with the incidence of crystallization increasing to 39.3% in mice lacking both proteins (Mo et al., 2004, 2007; Wesson et al., 2003). These findings indicate that OPN and THP act cooperatively to limit CaOx crystal formation and tissue retention *in vivo* (Mo et al., 2004, 2007; Wesson et al., 2003).

OSM: OSM is an IL-6 family cytokine implicated in renal inflammation and disease progression (Hermanns, 2015). Yamashita et al. (2020) used OSMRβ-knockout mice to define the contribution of OSM signaling to renal crystallization and showed that OSM may act directly on renal tubular epithelial cells and fibroblasts to induce crystallization-related molecules and inflammatory cytokines, thereby promoting intrarenal crystal aggregation. Subsequent work evaluated the preventive potential of OSMRβ pathway blockade using anti-OSMRβ monoclonal antibodies in an acetaldehyde-induced renal crystallization model; this treatment significantly reduced intrarenal crystal deposition and suppressed crystallization-associated proteins, the tubular injury marker KIM-1, and inflammatory and profibrotic factors (Deguchi et al., 2024; Yamashita et al., 2020).

FABP4: Although epidemiological and clinical evidence has linked obesity to kidney stone risk, the mechanisms connecting disordered lipid metabolism to CaOx stone formation remain unclear (Lee et al., 2008; Taylor et al., 2005). RNA sequencing of renal papillary tissue containing Randall's plaques revealed lipid metabolic dysregulation associated with reduced FABP4 expression, suggesting altered fatty acid handling in papillary microenvironment remodeling (Taguchi et al., 2020). Consistent with this association, CaOx crystals have been detected in FABP4-deficient mice, supporting a protective role for FABP4 against crystal deposition (Taguchi et al., 2020).

FKBP5: FKBP5 has emerged as a promising candidate biomarker of kidney injury; however, its precise functional contribution to CaOx nephrolithiasis remains incompletely defined. Song et al. (2023) manipulated FKBP5 expression using lentiviral and adeno-associated viral vectors in a murine stone model and found that genetic deletion markedly reduced renal crystal aggregation, alleviated kidney injury, and decreased crystal adhesion to renal cells, suggesting that FKBP5 contributes to crystal retention and tissue damage during CaOx nephrolithiasis.

Androgen receptor (AR): Kidney stones occur more

Table 1 Summary of CaOx stone and gene knockout models in mice

Mouse	Diet/Administration	Effects	References
C57BL/6	Diet containing 1.5% NaOx for two weeks	Hyperoxaluria	Hanstock et al., 2024
		Renal CaOx crystal deposition in outer medulla cortical tubules	
C57BL/6	Daily intraperitoneal injections of GOX for 7 days		Okada et al., 2007
	50 mg/kg	Absence of CaOx crystals	
	60 mg/kg	40% CaOx crystals, mainly in renal tubules located at border between renal cortex and medulla	
	80 mg/kg	100% CaOx crystals, mainly in renal tubules located at border between renal cortex and medulla	
	150 mg/kg	Mortality	
C57BL/6JNarl	Daily intraperitoneal injections of GOX (100 mg/kg) for 5 to 7 days	Hyperoxaluria CaOx crystals, mainly in renal tubules located at border between renal cortex and medulla	Liu et al., 2025
C57BL/6J	Daily intraperitoneal injections of GOX (80 mg/kg) for 6 consecutive days, combined with dorsal implantation of anti-OSMRβ antibody	Significantly attenuated renal crystal deposition	Deguchi et al., 2024
Npt2a KO	EG, GOX, or HLP for 4 weeks	Hyperoxaluria Renal CaOx crystal deposition in outer medulla and cortical tubules Intratubular CaP crystal deposition	Khan & Glenton, 2010
OPN KO	1% EG for 4 weeks	Hyperoxaluria Intratubular CaOx crystal deposition	Wesson et al., 2003
RXRα KO	Daily intraperitoneal injections of GOX (70 mg/kg) Daily intraperitoneal injections of GOX (80 mg/kg)	Hyperoxaluria Intratubular CaOx crystal deposition Mortality	Yang et al., 2025
OSMRβ KO	Daily intraperitoneal injections of GOX (80 mg/kg) for 3, 6, or 9 consecutive days	Markedly reduced renal crystal deposition	Yamashita et al., 2020
FABP4 KO	Daily intraperitoneal injections of GOX (80 mg/kg) for 6 consecutive days	Significantly increased renal crystal deposition and urinary crystal excretion	Taguchi et al., 2020
FKBP5 KO	Renal pelvic injection of AAV-sh-FKBP5 Daily intraperitoneal injections of GOX (80 mg/kg) for 6 consecutive days	Attenuated renal stone aggregation and tubular injury, and reduced infiltration of M1-type inflammatory macrophages in kidney	Song et al., 2023
AR KO	Daily intraperitoneal injections of GOX (80 mg/kg) for 6 consecutive days	Reduced renal CaOx crystal deposition	Zhu et al., 2019
PRMT1 KO	Daily intraperitoneal injections of GOX (100 mg/kg) for 10 consecutive days	Reduced renal CaOx crystal deposition	Yuan et al., 2025
Abcc6 KO	Normal	Spontaneous apatite calcification in renal papillary interstitium with aging, localized at papillary tip and surrounding loops of Henle and vasa recta, resembling human Randall's plaques. Urinary PPi excretion significantly reduced	Letavernier et al., 2018
Slc26a1KO	Normal	Hyperoxaluria	Dawson et al., 2010
		Hyperoxalemia	
		CaOx stones in renal cortical tubules and bladder	
Slc26a6 KO	Normal	Hyperoxaluria	Jiang et al., 2006
		Hyperoxalemia	
Slc26a3 KO	Normal	Significantly reduced urinary and serum oxalate concentrations	Freel et al., 2013
THP KO	Normal	Spontaneous calcium crystals in renal collecting ducts and papillae in 16% of mice	Mo et al., 2004
	Drinking water with 1% EG and 4 IU/mL vitamin D3 for 1 month	Extensive CaOx crystal formation in kidneys in 76% of mice, particularly in outer medulla	

AR: Androgen receptor; CaOx: Calcium oxalate; CaP: Calcium phosphate; EG: Ethylene glycol; FABP4: Fatty-acid binding protein 4; FKBP5: FKBP prolyl isomerase 5; GOX: glyoxylate, HLP: hydroxy-L-proline, KO: knockout, M1: macrophage-1, NaOx: sodium oxalate, Npt2a: IIa sodium-phosphate cotransporter, OPN: osteopontin, OSMRβ: OSM receptor β, PPi: proton pump inhibitors, PRMT1: protein arginine methyltransferase 1, THP: Tamm-Horsfall protein.

frequently in males than in females, indicating that sex hormone signaling may influence disease susceptibility through hormone receptor-mediated pathways (Li et al., 2010; Naghii et al., 2014; Zeng et al., 2017). In male patients, AR signaling is elevated and can promote hepatic oxalate biosynthesis while enhancing oxidative stress in renal tissue, thereby exacerbating CaOx crystal deposition (Chen et al., 2001; Liang et al., 2014). In a glyoxylate-induced model, tubule-specific AR-knockout mice showed markedly reduced renal CaOx deposition compared with wild-type mice,

indicating a critical role of tubular AR signaling in crystal development (Zhu et al., 2019).

PRMT1: PRMT1 is a key epigenetic regulatory enzyme that catalyzes arginine methylation and participates in renal metabolic reprogramming (Nicholson et al., 2009; Thiebaut et al., 2021; Yuan et al., 2025). Although the mechanistic role of PRMT1 in CaOx nephrotoxicity is currently unclear, recent evidence indicates that PRMT1 regulates fatty acid metabolism and links metabolic remodeling to renal injury (Guertin & Sabatini, 2007; Ye et al., 2024; Zhu et al., 2022). Notably, studies using mouse models with PRMT1-specific deletion or overexpression have reported that PRMT1 promotes ubiquitin-mediated degradation of peroxisome proliferator-activated receptor γ (PPARγ) through arginine methylation, thereby impairing fatty acid metabolism and exacerbating CaOx crystal-induced renal injury (Yuan et al., 2025).

Together, these genetic models identify urinary crystal inhibitors, inflammatory cytokine pathways, lipid metabolic regulators, injury-associated proteins, sex hormone signaling, and epigenetic control of metabolism as potential therapeutic targets for calcium oxalate kidney stone disease.

Randall's plaque model

Randall's plaques are subepithelial or interstitial CaP deposits that arise within the basement membranes of thin loops of Henle and vasa recta in the renal papilla, where they can provide an anchoring platform for CaOx crystal attachment and stone overgrowth (Daudon et al., 2015; Evan et al., 2007; Khan et al., 2012, 2021; Randall, 1936). Randall's plugs represent a related but mechanistically distinct lesion characterized by intratubular crystal occlusion, which may extend into the papillary ductal lumen and contribute to stone nucleation (Daudon et al., 2015; Khan et al., 2021; Worcester & Coe, 2010). Most chemically induced CaOx models primarily reproduce tubular crystal retention or plugging rather than the interstitial mineralization process that defines true plaque biology (Daudon et al., 2015; Khan & Glenton, 2010; Liu et al., 2025; Okada et al., 2007; Tzou et al., 2016). Among plaque-related models, Abcc6-deficient mice spontaneously develop age-dependent interstitial hydroxyapatite calcification at the papillary tips, with lesions that closely resemble major morphological features of human papillary hydroxyapatite calcification (Letavernier et al., 2018, 2019). Vitamin D and calcium supplementation can accelerate papillary calcification in Abcc6-knockout mice, thereby improving experimental access to the plaque phenotype for mechanistic studies (Bouderlique et al., 2019). Nevertheless, Abcc6-knockout mice do not consistently develop CaOx overgrowth on plaques or spontaneous stone passage into the collecting system, and plaque-to-stone transition often requires additional urinary supersaturation (Daudon et al., 2015; Khan et al., 2021; Letavernier et al., 2018, 2019). Therefore, Abcc6 knockout is best interpreted as a model of interstitial plaque initiation and expansion rather than a complete model of CaOx nephrolithiasis (Bouderlique et al., 2019; Letavernier et al., 2018, 2019). The plaque and plug pathways are shown in Figure 3A and Figure 3B, respectively.

Type IIa sodium-phosphate cotransporter (NaPi-IIa), encoded by SLC34A1, is predominantly expressed on the brush-border membrane of renal proximal tubular cells and mediates phosphate reabsorption (Tenenhouse, 2005). In NaPi-IIa-knockout mice, increased urinary phosphate and calcium loss was accompanied by CaP deposition in tubular

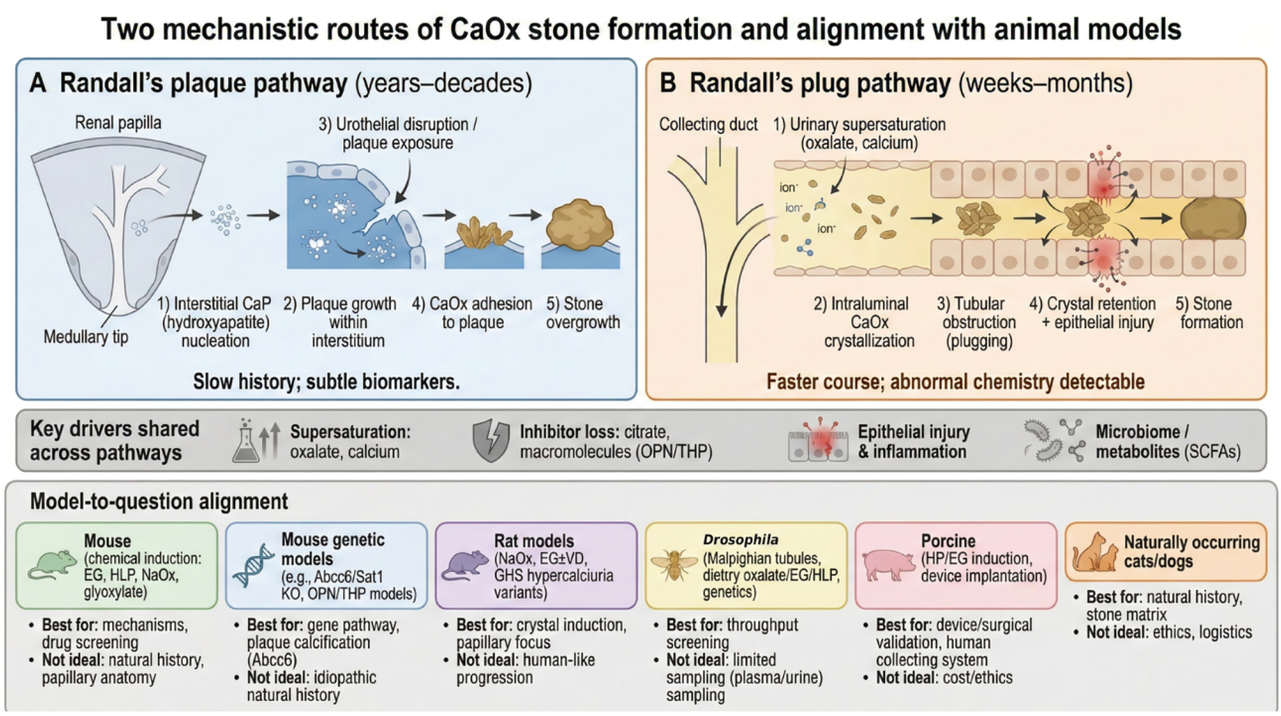

Figure 3 Two mechanistic routes of CaOx stone formation and alignment with animal models

A: Randall's plaque pathway (years to decades): Interstitial CaP (hydroxyapatite) nucleation and plaque growth within the papillary interstitium, followed by urothelial disruption, plaque exposure, CaOx adhesion, and stone overgrowth. B: Randall's plug pathway (weeks to months): Urinary supersaturation drives intraluminal CaOx crystallization, tubular obstruction, epithelial injury, crystal retention, and stone formation. Shared drivers, including supersaturation, loss of inhibitors, epithelial injury, inflammation, microbiome changes, and metabolites, are indicated. The bottom panel aligns representative animal models with the mechanistic route and most appropriate research questions, including mechanistic studies, drug screening, plaque-relevant calcification, long-term progression, and translational or device evaluation.

and interstitial compartments (Khan & Glenton, 2008). Although these findings suggest a potential connection between SLC34A1 dysfunction and Randall's body-like calcification, current evidence is insufficient to establish a direct role for SLC34A1 in Randall's plaque formation.

To enhance reproducibility and clinical relevance, plaque and plug models should be reported with standardized urinary chemistry parameters, such as oxalate, calcium, citrate, pH, urine volume, and supersaturation, as well as stone location, induction duration, recovery interval, and off-target toxicity (Khan & Glenton, 2010; Tzou et al., 2016). Where appropriate, secondary stimuli such as controlled dietary calcium intake, dehydration, or microbiome disruption should be incorporated according to the intended human mechanism. Readouts should also distinguish plaque formation from plugging to avoid overinterpretation of intratubular crystal retention as complete stone disease (Daudon et al., 2015; Hanstock et al., 2024; Jung et al., 2023; Khan & Glenton, 2010; Kok et al., 2017; Tzou et al., 2016).

Research advances in drug development

Mouse CaOx models have supported preclinical evaluation of diverse candidate interventions for kidney stone prevention and treatment, including hesperidin, gallic acid, theaflavin, rutin, umbelliferone, tartronic acid, *Pelvetia siliquosa* polysaccharides (PSPs), and short-chain fatty acids (SCFAs) (Chen et al., 2025; Jin et al., 2021; Liu et al., 2021b; Kale et al., 2024; Su et al., 2024b; Xu et al., 2025; Ye et al., 2021; Zhang et al., 2025; Zhou et al., 2022). Further details are provided in Table 2.

NaOx-induced urolithiasis mouse models have been used to evaluate the anti-urolithiasis activity of plant components, with hesperidin shown to reduce multiple serum and urinary indices associated with stone formation (Kale et al., 2024). Furthermore, kidney stone mouse models have been established through repeated intraperitoneal injections of glyoxylate, with gallic acid found to protect against renal stone deposition and subsequent tubular injury (Zhou et al., 2022). Other compounds have also shown activity through antioxidant, anti-apoptotic, or anti-inflammatory mechanisms. For example, rutin alleviates CaOx crystal deposition, renal tissue damage, and crystallization-associated apoptosis in a glyoxylate-induced stone model (Zhang et al., 2025). Theaflavin exhibits strong renal protection by restoring miR-128-3p/SIRT1 axis-regulated antioxidant defense and reducing CaOx-induced renal injury (Ye et al., 2021). Umbelliferone also reduces renal crystal deposition and mitigates associated inflammation and tissue injury in cellular and mouse models of CaOx nephrocalcinosis (Xu et al., 2025).

Gut microbiota-derived metabolites have provided an additional therapeutic direction. SCFAs, key metabolites generated through microbial fermentation of dietary fiber, have potent immunomodulatory functions (Duscha et al., 2020; Fachi et al., 2020; Lavelle & Sokol, 2020). Recent studies have indicated that SCFAs are associated with CaOx stone pathogenesis and can suppress stone development in glyoxylate-induced mouse models through a GPR43-dependent immunomodulatory mechanism (Jin et al., 2021; Liu et al., 2021b).

Crystal growth modifiers also remain important anti-stone candidates. Citric acid inhibits kidney stone formation partly by suppressing COM crystal growth (Chung et al., 2016; Farmanesh et al., 2014; Ma et al., 2020; Rimer et al., 2010; Weissbuch & Leiserowitz, 2008). In contrast, tartaric acid binds preferentially to the active surface at the rapidly growing apex of CaOx crystals but achieves therapeutic efficacy comparable to that of citric acid (Su et al., 2024b). In another hyperoxaluric mouse model, PSP administration reduced CaOx crystal deposition and down-regulated CD44 and OPN expression, suggesting that marine polysaccharides may limit both crystal retention and injury-associated matrix responses (Chen et al., 2025).

Together, these studies highlight mouse CaOx models as useful platforms for identifying candidate therapies that target urinary chemistry, crystal growth, oxidative injury, inflammation, microbiome-derived signaling, and crystal adhesion.

Prospects

Mouse models offer important practical advantages for CaOx stone research, including short induction periods, genetic tractability, low maintenance cost, and suitability for mechanistic studies and early-stage drug screening. However, their translational value is constrained by simplified renal papillary anatomy, differences in nephron architecture compared with humans, and the frequent reliance on chemical inducers such as EG or glyoxylate, which can produce renal injury that is not specific to stone pathogenesis. In addition, many patients with CaOx stones do not present with marked hyperoxaluria, whereas most mouse models depend on experimentally induced oxalate overload. These limitations mean that mouse models should not be treated as direct replicas of human CaOx stone disease. Instead, their use should be matched to defined experimental aims, with careful distinction between crystal deposition, nephrocalcinosis, tubular plugging, plaque-related mineralization, and clinically relevant stone formation.

RAT MODELS

Rats remain among the most frequently used experimental animals in urinary stone research, particularly for modeling CaOx nephrolithiasis through induced hyperoxaluria or combined hyperoxaluria and hypercalciuria (Alexander et al., 2022; Khan et al., 2021; Singh et al., 2022; Tzou et al., 2016). In addition to metabolic induction, recent evidence has indicated that bacterial infection may also contribute to CaOx stone development (Cherng et al., 2019). Rat CaOx stone models are detailed in Table 3.

Comparison of rat and human kidneys

Important anatomical differences between rat and human kidneys constrain direct translation of rat stone phenotypes to human disease (Khan, 1997). Rat kidneys are much smaller, contain a single renal papilla, possess fewer ureteric ducts, feature a simpler renal pelvic architecture, and have relatively narrower ureteral lumens than human kidneys (Khan, 1997). Human kidneys are substantially larger and structurally more complex than rat kidneys, measuring approximately 12×6×4 cm and weighing 160–175 g, compared with 1.6×1.0×0.9 cm and 0.75–1.20 g in rats. Humans also have approximately 5–6 renal papillae and 850 000–1 200 000 nephrons per kidney, whereas rats have a single renal papilla and approximately 30 000–31 000 nephrons per kidney (Khan, 1997).. Despite these scale and structural differences, the medulla-to-cortex volume ratio is very similar between the two species (1:2) (Khan, 1997).

CaOx stone models

Oxalate metabolism is broadly conserved between rats and

Table 2 Summary of drug development in animal models

Animal model	Method	Intervention	Mechanism	References
Mouse	70 mg/kg NaOx for 7 days	Hesperidin	Diuresis Inhibition of crystallization	Kale et al., 2024
	Daily intraperitoneal injections of GOX (75 mg/kg) for 6 consecutive days	GAL	Up-regulation of Nrf2/HO-1 signaling Suppression of OPN and its receptor CD44 Attenuation of renal macrophage infiltration	Zhou et al., 2022
	Daily intraperitoneal injections of GOX (75 mg/kg) for 7 consecutive days	TF	Inhibition of miR-128-3p/SIRT1 axis	Ye et al., 2021
	Daily intraperitoneal injections of GOX (80 mg/kg) for 6 consecutive days	Rutin	Attenuation of oxidative stress Inhibition of apoptosis Suppression of NF-κB pathway Promotion of SCFA production	Zhang et al., 2025
	Daily intraperitoneal injections of GOX (100 mg/kg) for 7 consecutive days	Umb	Activation of PI3K/AKT pathway	Xu et al., 2025
	Daily intraperitoneal injections of GOX for 14 consecutive days	Tartronic acid	Interaction with fast-growing apical surface of COM crystals to inhibit growth	Su et al., 2024b
	Daily intraperitoneal injections of GOX (70 mg/kg) for 7 consecutive days	PSPs	Chelation of Ca^{2+} via sulfate groups, suppressing CaOx nucleation and growth Up-regulation of SOD/CAT activity, reducing ROS and oxidative injury Down-regulation of inflammatory factor and adhesion protein (CD44, OPN) expression	Chen et al., 2025
	Daily intraperitoneal injections of GOX (80 mg/kg) for 7 consecutive days	SCFAs	Suppression of calculogenesis via GPR43-dependent immunomodulation and anti-inflammatory actions	Jin et al., 2021
Rat	Drinking water containing 1% EG for 28 consecutive days	Succinate	Reduction of renal calcium deposition and injury Inhibition of cellular adhesion and osteogenic differentiation Down-regulation of CD44, IL-6, and OPN expression	Zhang et al., 2023
	Drinking water containing 1% EG for 28 consecutive days	Glycine	Down-regulation of Slc26a6 Down-regulation of Nadc1 Up-regulation of miR-411-3p	Lan et al., 2021
	Drinking water containing 1% EG for 28 consecutive days	Yellow tea	Activation of PPARγ pathway with subsequent attenuation of oxidative stress and suppression of EMT and renal fibrosis	Su et al., 2023
	Drinking water containing 0.75% EG for 28 consecutive days	Selenium	Up-regulation of selenoprotein K and suppression of IRE1-ASK1-JNK pathway, attenuating endoplasmic reticulum stress and apoptosis	Su et al., 2024a
	Drinking water containing 0.4% NH_4Cl and 1% EG	Zinc	Enhancement of oxalate decarboxylase activity and stability with promotion of *Lactobacillus* growth to potentiate oxalate metabolism	Wu et al., 2023
	Sodium-deficient diet (0.006% sodium) combined with a 0.75% EG solution for 42 days	Sodium	Down-regulation of renal sodium transporters and aquaporins Increased urinary calcium excretion and CaOx supersaturation	Huang et al., 2024
	Drinking water containing 1% EG for 4 weeks	SCFAs	Up-regulation of SLC26A6 Down-regulation of SLC26A3	Liu et al., 2020
	Drinking water containing 1% EG for 4 weeks	*Lactiplantibacillus plantarum J-15*	Up-regulation of Occludin Suppression of renal TLR4/NF-κB/COX-2 signaling	Tian et al., 2022
Drosophila	0.1% NaOx solution for 7 days	HH, DS, HQ	Inhibition of crystallization Attenuation of oxidative stress Enhancement of diuresis	Ren et al., 2025
	0.2% NaOx	Water extracts and 50% ethanol extracts of 46 Chinese herbal medicines	Inhibition of CaOx crystal formation and deposition in MTs	Lu et al., 2024
	0.5% EG for 3 weeks	*Astragalus membranaceus*	Prophylactic suppression of crystal formation in MTs	Chen et al., 2022a
	0.3% NaOx solution for 7 days	*Garcinia cambogia*	Chemical dissolution of CaOx stones	Fan et al., 2020
	0.1% oxalic acid	AOFOS	Suppression of macroscopic crystallization Attenuation of CaOx crystallization kinetics Modulation of crystal phase transition (COM-to-COD)	Sun et al., 2024
	0.1% NaOx	*Bacillus subtilis 168*, *BS168*	Modulation of gut microbiota	Al et al., 2020

AOFOS: *Aspidopterys obcordata* fructo-oligosaccharide, CaOx: calcium oxalate, COD: calcium oxalate dihydrate, COM: calcium oxalate monohydrate, DS: Danshen, EG: ethylene glycol, EMT: epithelial-mesenchymal transition, GAL: gallic acid, GOX: glyoxylate, HH: Honghua, HLP: hydroxy-L-proline, HQ: Huangqi, KO: knockout, MT: Malpighian tubules, NaOx: sodium oxalate, OPN: osteopontin, PSPs: *Pelvetia siliquosa* polysaccharides, SCFAs: short-chain fatty acids, TF: theaflavin, Umb: umbelliferone.

Table 3 Summary of CaOx stone models in rats

Type of approach	Lithogenic agent, references	Diet/Administration	Effects
Infection	*Proteus mirabilis* (Cherng et al., 2019)	Intravesical instillation of saline containing 1×10^7 CFU proteus mirabilis+surgical implantation of a 2-mm polyethylene tube into bladder	Stone deposition observed in bladder and kidneys Significant time-dependent down-regulation of MCP-1, OPN, and TRPV5 expression in renal tissue
Chemical induction	NaOx (Khan et al., 1982)	Intraperitoneal injection	Hyperoxaluria CaOx crystal deposition CaOx microcalculi
	EG+Vitamin D3 (de Water et al., 1996; Lyon et al., 1966)	Dietary EG (0.5%, 0.75%, 1.0%, 1.5%) and vitamin D3 for 4 consecutive weeks	0.5% EG group: Only partial rats exhibited CaOx deposition in renal cortex and/or medulla ≥0.75% EG groups: All rats developed CaOx crystal formation
	Glycolic acid (Ahsan et al., 1989; Ogawa et al., 1986, 1990)	3% glycolic acid for 4 consecutive weeks	CaOx crystal deposition
	HLP (Khan et al., 2006; Tawashi et al., 1980; Thomas et al., 1971)	Single intraperitoneal injection of 2.5 g/kg HLP	Hyperoxaluria CaOx crystal deposition
Inbreeding	Inbreeding hypercalciuric progeny (Bushinsky et al., 2002; Krieger et al., 2021)	Standard diet containing 1.2% calcium for 18 weeks+HLP Base diet+5% HLP	Hyperoxaluria CaP crystal deposition CaOx crystal deposition

CaOx: calcium oxalate, CaP: calcium phosphate, EG: ethylene glycol, HLP: hydroxy-L-proline. KO: knockout, MCP-1: monocyte chemotactic protein-1, NaOx: sodium oxalate, OPN: osteopontin, TRPV5: transient receptor potential vanilloid 5.

humans, and experimentally induced renal calculi in rats reproduce several processes relevant to human kidney stone development (Khan, 1997). Consequently, rat models remain important platforms for investigating CaOx nephrolithiasis. Currently, most rat models are generated through exogenous lithogenic agents, including NaOx, EG, glycolic acid, and HLP (Tzou et al., 2016). Recent research also suggests that bacterial infection may promote CaOx stone development under specific inflammatory conditions (Cherng et al., 2019).

Bacterial models of CaOx stone development: Bacterial infection is a well-established driver of struvite stones, but its contribution to CaOx formation remains less clear (Khan et al., 2016; Worcester & Coe, 2010). Infection-associated inflammation, biofilm formation, and epithelial injury can modify urinary macromolecules and alter the local nucleation microenvironment (Cherng et al., 2019; Khan et al., 2021). Current evidence supports the possibility that infection acts as a synergistic factor for CaOx crystal retention rather than as an independent primary cause (Cherng et al., 2019). Given the limited direct causal evidence linking infection to idiopathic CaOx nephrolithiasis, infection-based models should be interpreted cautiously. These models are more suitable for studying mixed calculi, inflammation-mediated crystal retention, and epithelial injury pathways rather than the spontaneous development of idiopathic CaOx stones (Cherng et al., 2019).

NaOx: A single intraperitoneal injection of NaOx induces progressive CaOx crystallization in rat kidneys, with deposits first emerging in the renal cortex, extending into the medulla and papillary tips, and later spreading from tubular lumens to intercellular spaces and the tubular cell-basement membrane interface (Khan et al., 1982). In contrast, continuous potassium oxalate (KOx) delivery through miniature osmotic pumps produces persistent crystalluria without overt renal pathology, with renal CaOx crystal deposition occurring only after additional intraperitoneal NaOx injection, likely reflecting a further increase in CaOx supersaturation within tubular fluid (Khan et al., 1979, 1983).

EG: EG combined with vitamin D3 provides a dose-responsive rat model of renal CaOx crystal deposition (de Water et al., 1996). At 0.5% EG, crystal deposition is minimal and limited to the renal cortex and/or medulla in only a subset of rats, whereas 0.75%, 1.0%, and 1.5% EG produce a dose-dependent increase in urinary oxalate and stable CaOx crystal formation across animals (de Water et al., 1996). However, EG-based induction requires careful toxicity control. When combined with NH_4Cl, EG can cause substantial weight loss and renal dysfunction (Blood, 1965; Eder et al., 1998; Yamaguchi et al., 2005), with concentrations above 1% associated with mortality rates as high as 61% in experimental rats (Lyon et al., 1966). Thus, EG-based rat models should include explicit dose optimization and toxicity assessment to distinguish lithogenic effects from nonspecific renal injury.

Glycolic acid: Glycolic acid is an oxalic acid precursor that significantly increases the incidence of CaOx stone formation (Runyan & Gershoff, 1965). Dietary supplementation with 3% glycolic acid reliably induces renal CaOx crystal development in rats (Ahsan et al., 1989; Ogawa et al., 1986, 1990). In Sprague-Dawley rats, glycolic acid treatment has been shown to increase kidney weight and promote calcium and oxalate deposition compared with normal controls (Ahsan et al., 1989), supporting its utility as a metabolic precursor-based model of oxalate-driven renal crystallization.

HLP: HLP induces CaOx nephrolithiasis in rats after intraperitoneal injection (Tawashi et al., 1980) and also produces a robust lithogenic phenotype when delivered through the diet. Notably, hyperoxaluria and crystalluria are significantly increased in HLP-fed rats, accompanied by widespread CaOx crystal deposition and stone formation throughout the kidney, particularly in collecting ducts and papillary tips (Khan et al., 2006), challenging earlier assumptions that HLP requires hypercalcemia to induce CaOx stone development (Tawashi et al., 1980; Thomas et al., 1971).

Enteric hyperoxaluria (malabsorptive) models: Enteric hyperoxaluria is a clinically significant cause of CaOx nephrolithiasis that develops when fat malabsorption increases intestinal oxalate absorption (Upala et al., 2016). Surgical rodent models, including Roux-en-Y gastric bypass, reproduce key features of malabsorptive stone risk, including

steatorrhea, altered intestinal oxalate handling, and increased urinary oxalate supersaturation (Kwenda et al., 2020). Unlike chemical hyperoxaluria models, these approaches reduce reliance on toxic oxalate precursors and provide a more etiologically suitable platform for studying interventions targeting the gut-kidney axis, such as dietary calcium, low-fat/low-oxalate diets, bile acid sequestrants, probiotics, and oxalate-degrading enzymes (Kwenda et al., 2020; Upala et al., 2016).

Genetic hypercalciuric stone-forming (GHS) rats

Hypercalciuria is a major risk factor for kidney stone disease and exhibits significant familial heritability (Bushinsky et al., 1995; Coe et al., 1992; Hoopes et al., 2003). GHS rat models have been generated through multigenerational selection of spontaneously hypercalciuric Sprague-Dawley rats, producing a stable model of inherited hypercalciuria (Bushinsky et al., 2002; Bushinsky & Favus, 1988). When maintained on a standard diet (1.2% calcium), GHS rats excrete urinary calcium at levels 8–10 times higher than control rats and uniformly develop CaP kidney stones (Bushinsky et al., 2002). This phenotype is notable because urinary CaOx supersaturation exceeds CaP supersaturation, yet untreated GHS rats form CaP rather than CaOx stones. HLP supplementation shifts this mineralization pattern by increasing urinary oxalate excretion and progressively increasing the CaOx-to-CaP supersaturation ratio, with 5% dietary HLP inducing CaOx stone development in GHS rats (Bushinsky et al., 2002). Regardless of whether CaP or CaOx stones form, crystal deposition occurs primarily within the urinary lumen, particularly near the renal pelvic outlet and around the solitary renal papilla in rats, rather than within renal tubules (Bushinsky et al., 2002).

GHS rats provide a tractable model for examining how inherited hypercalciuria interacts with oxalate loading to shift lithogenesis from CaP-dominant to CaOx-dominant stone formation. Extending this approach, Krieger et al. (2021) established a genetic hypercalciuric rat model relevant to human idiopathic hypercalciuria, in which all rats developed CaOx stones and combined clonazepam and potassium citrate therapy reduced stone formation and improved bone quality more effectively than either treatment alone.Additional hypercalciuric rat studies have shown that calcium and vitamin D act synergistically to promote stone development, dietary magnesium reduces urinary supersaturation without decreasing CaOx stone formation, and high-casein feeding links excessive animal protein intake to coordinated renal and skeletal alterations that contribute to hypercalciuria (Amanzadeh et al., 2003; Letavernier et al., 2016; Li et al., 2024).

Research advances in drug development

Similar to mouse models, rat models have been used to evaluate metabolic, nutritional, microbial, and pharmacological interventions with potential relevance to kidney stone treatment, including succinate, glycine, PPARγ agonists, selenium, zinc, sodium, SCFAs, and *Lactiplantibacillus plantarum* strains (Huang et al., 2024; Koh et al., 2016; Lan et al., 2021; Liu et al., 2021a; Su et al., 2023, 2024a; Tian et al., 2022; Wu et al., 2023, 2025; Zhang et al., 2023). Further details are provided in Table 2.

Succinate: Succinate, a tricarboxylic acid (TCA) cycle intermediate, has been shown to reduce CaOx crystal nucleation *in vitro* and renal CaOx deposition in EG-induced rats, with these protective effects associated with attenuated inflammation, reduced crystal-cell adhesion, and suppressed osteogenic differentiation (Zhang et al., 2023).

Glycine: Glycine has been shown to reduce CaOx crystal development in rats by regulating urinary oxalate and citrate handling. Mechanistically, glycine promotes miR-411-3p-mediated down-regulation of SLC26A6 and NaDC1 protein expression, thereby lowering urinary oxalate and increasing urinary citrate (Lan et al., 2021).

Yellow tea: Yellow tea infusion has been shown to reduce renal crystal deposition in an EG-induced rat stone model, with flavonoid components regulating PPARγ protein activity and thereby influencing stone development (Su et al., 2023). Consistent with this metabolic regulatory axis, the PPARγ agonist pioglitazone has also been reported to decrease CaOx crystal deposition, potentially through lipid metabolism modulation (Wu et al., 2025).

Selenium: Selenomethionine (SeMet) has been evaluated in complementary CaOx stone models established using HK-2 cells and EG-gavaged Sprague-Dawley rats, with SeMet treatment shown to significantly alleviate oxidative damage, endoplasmic reticulum (ER) stress, and programmed cell death, thereby protecting renal tubular epithelial cells from crystal-induced damage (Su et al., 2024a).

Zinc: Zinc gluconate has been shown to enhance colonization by *Oxalobacter formigenes* in patients with CaOx stones, activate the lactic acid bacteria-oxalate decarboxylase (OxDC) system, and reduce stone progression, with Zn^{2+} promoting both OxDC activity and lactic acid bacterial proliferation (Wu et al., 2023).

Sodium: Long-term sodium restriction has been reported to reduce urinary sodium excretion but paradoxically induce hypercalciuria and renal dysfunction, thereby promoting CaOx crystal development and exacerbating kidney stone formation in rats (Huang et al., 2024).

SCFAs: SCFAs are gut microbiota-derived metabolites generated through dietary fiber fermentation, but humans lack the capacity for direct SCFA synthesis (Koh et al., 2016). Patients with kidney stones demonstrate a markedly lower abundance of SCFA-producing gut bacteria than healthy individuals (Liu et al., 2020). In rat models, SCFAs reduce urinary oxalate levels and renal CaOx stone development by promoting SLC26A6-mediated oxalate excretion (Liu et al., 2021a), supporting a microbiota-dependent mechanism for oxalate homeostasis.

Lactiplantibacillus plantarum: *Lactiplantibacillus plantarum* strains *N-1* and *J-15* have shown significant preventive potential against CaOx stone formation (Liu et al., 2021b; Tian et al., 2022). The *N-1* strain significantly reduces renal CaOx crystal deposition by reshaping gut microbiota composition and regulating arginine metabolism (Liu et al., 2021b). The *J-15* strain acts through restoration of microbial community structure, correction of metabolic disturbances, and enhancement of intestinal barrier function (Tian et al., 2022).

Prospects

Rats remain the most widely used model for CaOx nephrolithiasis due to their cost-effectiveness, adaptability, and suitability for repeated urine collection for longitudinal biochemical assessment. However, many rat models still rely on acute hyperoxaluria and primarily generate intratubular crystals rather than true renal pelvic stones. Improving translational relevance will require model selection based on human etiological characteristics, including enteric, genetic, and pH-related mechanisms; standardized reporting of urinary

chemistry and supersaturation; precise anatomical localization using quantitative imaging and histopathology; and careful control of renal toxicity during combined drug administration.

DROSOPHILA MODELS

Drosophila melanogaster provides an efficient, low-cost, and genetically tractable model for kidney stone research, combining rapid husbandry, extensive mutant resources, mature transgenic technology, and fewer regulatory constraints than mammalian systems (Dow et al., 2022; Tzou et al., 2016).

Structure and function of *Drosophila*

The excretory system of *Drosophila* is centered on Malpighian tubules (MTs), which demonstrate remarkable architectural and physiological conservation with mammalian nephrons (Miller et al., 2013; Reynolds et al., 2021; Wang et al., 2022). Most mammalian renal proteins have clear homologs in *Drosophila*, which often retain conserved functions relevant to epithelial transport, solute handling, and renal injury responses (Reynolds et al., 2021). In *Drosophila*, excretory homeostasis depends on coordinated activity among MTs, which mediate secretion and excretion; the hindgut, which contributes to reabsorption; and nephrocytes, which perform filtration-associated endocytosis (Dow et al., 2022). Various genes essential for mammalian kidney function have direct functionally active homologs in *Drosophila* kidney tissues, enabling studies of epithelial transport, nephrolithiasis, podocyte-like filtration, and proximal tubule-associated processes (Dow et al., 2022). Adult *Drosophila* MTs show limited cellular renewal, providing a useful system for investigating rapid fluid transport, neuroendocrine regulation of renal physiology, and kidney pathologies such as nephrolithiasis (Cohen et al., 2020; Wang & Spradling, 2020). However, like mammalian kidneys, MTs are susceptible to crystal-associated damage, supporting their use in stone-related injury models (Cohen et al., 2020; Wang & Spradling, 2020).

CaOx stone models

CaOx crystallization models in *Drosophila* have been established through both dietary lithogenic stimuli and genetic manipulation techniques. Further details are provided in Table 4.

Diet-induced models: Chen et al. (2011) successfully established a *Drosophila* CaOx crystallization model using a two-week diet supplemented with EG, HLP, or NaOx, with treatment producing dose-dependent CaOx crystal accumulation in MTs. These agents increase oxalate availability through distinct routes: EG is metabolized into oxalate *in vivo*, NaOx provides direct dietary oxalate, and HLP generates oxalate through hydroxyproline-to-glyoxylate metabolism via the HOG pathway (Buchalski et al., 2020; Ermer et al., 2023; Wang et al., 2022). Despite these mechanistic differences, all three stimuli increase CaOx crystal risk by raising oxalate burden (Buchalski et al., 2020; Ermer et al., 2023; Wang et al., 2022).

Genetic manipulation model: Yang et al. (2018) generated a *Drosophila* CaOx kidney stone model by functionally down-regulating dAGXT. dAGXT encodes alanine-glyoxylate transaminase (AGT), which catalyzes transamination between L-alanine and glyoxylate (Wang et al., 2022). Reduced AGT activity disrupts glyoxylate detoxification, causing glyoxylate accumulation and subsequent conversion to oxalate by oxidizing enzymes such as lactate dehydrogenase, with increased systemic oxalate ultimately precipitating CaOx crystals within the MT lumen (Wang et al., 2022).

Additional work has identified OPN-derived peptides, dPrestin (Slc26a6), and Neat as regulators of CaOx crystallization in *Drosophila* models (Akouris et al., 2022; Landry et al., 2016; Rossano et al., 2025). Notably, Akouris et al. (2023) first demonstrated in a *Drosophila melanogaster* model that phosphorylated OPN peptide segments can directly reduce CaOx urinary stone development *in vivo* by altering crystal morphology. dPrestin (Slc26a6) mediates apical oxalate secretion into the lumen, whereas Neat functions as a principal basolateral oxalate transporter, with its knockout shown to markedly reduce CaOx crystal development in the MTs (Rossano et al., 2025). Sulfate and thiosulfate have also been reported to suppress oxalate transport through a dPrestin-dependent pathway (Landry et al., 2016).

Research advances in drug development

As a rapid and genetically tractable system, *Drosophila* models have become useful tools for early-stage anti-stone drug discovery. Dietary lithogen-induced CaOx crystallization in the MTs has been particularly valuable for screening candidate interventions, including medicinal plant extracts, organic acids, polysaccharides, and probiotics (Wang et al., 2022; Al et al., 2020; Chen et al., 2022a; Fan et al., 2020; Kale et al., 2024; Lu et al., 2024; Ren et al., 2025; Sun et al., 2022).

Table 4 Summary of CaOx stone models in *Drosophila*

References	Model/Protein	Diet/Intervention	Effects
Chen et al., 2011	Diet-induced model	0.5% EG	CaOx crystals in MTs
		0.01%–1% HLP	
		0.01%–0.05% NaOx	
Yang et al., 2018	Genetic manipulation model	dAGXT KO	CaOx crystals in MTs
Akouris et al., 2022	OPN	0.1% NaOx Oral administration of 2 000 μg/mL OPN phosphopeptide	Significantly reduced CaOx stones Decreased crystal adhesion to renal epithelial cells
Rossano et al., 2025	Neat	10 mM NaOx+Neat KO	Significantly reduced CaOx stones
Landry et al., 2016	dPrestin	5 mM NaOx+20 mM sulfate/thiosulfate diet+dPrestin KO	Significantly reduced CaOx crystals within 24 h of thiosulfate Efficacy 48 h after sulfate. Inhibition disappears after dPrestin KO

CaOx: Calcium oxalate, EG: ethylene glycol, HLP: hydroxy-L-proline, KO: knockout, MT: Malpighian tubules, NaOx: sodium oxalate, OPN: osteopontin.

Further details are provided in Table 2.

Ren et al. (2025) established a *Drosophila* renal calculus model by inducing MT crystallization through NaOx administration and used this system to evaluate three traditional Chinese medicines, Honghua (HH), Danshen (DS), and Huangqi (HQ), selected from 15 candidate substances. Kale et al. (2024) used a NaOx-induced *Drosophila* urinary calculus model to show that hesperidin improved calculus-related physiological indicators, supporting its potential as an anti-urolithiasis candidate. In a separate 0.2% NaOx feeding model, Lu et al. (2024) screened botanical extracts and identified 24 water extracts with anti-lithiasis activity, including five candidates with low toxicity, as well as eight ethanol extracts that showed therapeutic efficacy. Using an EG-induced *Drosophila* model, Chen et al. (2022a) reported that *Astragalus* extract reduced CaOx crystal formation in the MTs and improved survival, with efficacy comparable to potassium citrate. Fan et al. (2020) further used wild-type and v-ATPase RNAi-knockout *Drosophila* fed a 0.3% NaOx diet to demonstrate that gamboge extract exerted direct crystal-dissolving litholytic activity, similar to hydroxycitric acid. AOFOS, an active polysaccharide from the Dai medicinal plant *Aspidopterys obcordata* Hemsl., reduced CaOx crystal size in a *Drosophila* kidney stone model by limiting large-crystal formation, slowing crystallization kinetics, and preventing COM-to-COD phase transformation (Sun et al., 2022, 2024). In another *Drosophila* stone model, *BS168* significantly reduced stone development, improved overall health status, and modulated gut microbiota composition (Al et al., 2020).

Prospects

Drosophila models offer major practical advantages for CaOx stone research, including short life cycle, low cost, efficient genetic manipulation, and suitability for high-throughput screening. MTs reproduce key aspects of calcium salt crystallization in renal tubular systems, supporting their use for mechanistic and pharmacological studies. However, these models have limited capacity to characterize tubular fluid dynamics or measure plasma and urinary biochemical parameters, reducing confidence in direct clinical translation of the resulting data (Knauf & Preisig, 2011).

PORCINE MODELS

Comparison between pigs and humans

Pigs are widely employed in biomedical research due to their anatomical and physiological resemblance to humans (Huang et al., 2021; Kim et al., 2022; Pique et al., 2018; Roth & Tuggle, 2015). This resemblance is particularly relevant in urology, as porcine kidneys share key structural and functional features with human kidneys (Bagetti Filho et al., 2008; Ren et al., 2022; Sampaio et al., 1998) and therefore provide a valuable platform for evaluating surgical approaches, device performance, and instrument safety (Amiel et al., 2025; Han et al., 2023; Rassweiler-Seyfried et al., 2023; Wei et al., 2024). Both species have polypapillary kidneys with broadly comparable calyceal organization and renal pelvic architecture (Golbaekdal et al., 1996; Hansen-Estruch et al., 2022). However, pig kidneys contain more nephrons than human kidneys, with approximately 1.6–4.6 million nephrons in pigs compared with 0.2–2.0 million in humans (Huang et al., 2021; Renner et al., 2020). Both species also have relatively short loops of Henle, although branching depth differs between cortical and outer medullary regions (Bankir et al., 2020). These anatomical similarities support the use of pigs for surgical and device evaluation; however, differences in concentration capacity and oxalate metabolism must be considered when modeling calculus pathophysiology.

CaOx kidney stone models

Porcine CaOx kidney stone models have been successfully established through surgical implantation of stones or exogenous administration of stone-inducing agents such as HLP and EG. Specific details are outlined in Table 5.

HLP: HLP feeding provides a practical dietary approach for inducing hyperoxaluria in pigs (Kaplon et al., 2010; Mandel et al., 2004; Patel et al., 2012; Sivalingam et al., 2013). Diets containing approximately 10% HLP have been shown to increase urinary oxalate to a plateau, with higher supplementation levels (e.g., 20%) not inducing further increases, suggesting saturable oxalate-generating metabolism (Kaplon et al., 2010). Crystals recovered from papillary tips typically contain COM and COD, and gross and histological analyses have shown macroscopic papillary crystal coverage with focal epithelial injury and inflammatory infiltration (Mandel et al., 2004). These features make HLP-fed pigs a useful bridge model for studying papillary crystal retention and evaluating safety endpoints, although the induced disease course remains far more rapid than the decades-long evolution of idiopathic stone formation in humans.

EG: EG-based porcine hyperoxaluria protocols have been developed, often with vitamin D or acid loading to enhance crystal deposition (Trojan et al., 2017). Across treatment regimens, CaOx crystals generally form within the renal parenchyma and are accompanied by inflammatory infiltration and functional alterations, including elevated blood urea nitrogen and creatinine levels, decreased urinary citrate, and reduced urine pH (Trojan et al., 2017). Among reported combinations, EG plus vitamin D produces robust crystal deposition with acceptable safety, whereas nephrotoxic co-treatments may confound interpretation (Trojan et al., 2017). Overall, EG-based porcine models are useful for studying crystal-induced injury and safety signals but primarily generate intrarenal deposits rather than true pelvic calculi.

Dietary oxalate: Porcine dietary oxalate models enable controlled manipulation of intestinal oxalate absorption through adjustment of oxalate load and dietary calcium-to-oxalate ratio (Penniston et al., 2017). High-oxalate or low-calcium diets increase urinary oxalate levels and CaOx crystalluria, whereas higher dietary calcium content reduces oxalate absorption by binding oxalate within the intestinal lumen (Penniston et al., 2017). These models are therefore well suited for studies of nutrition-dependent oxalate handling and gut-kidney axis mechanisms, but, similar to other induction approaches, they primarily yield crystalluria or crystal deposition endpoints rather than spontaneous pelvic stone formation.

Porcine models for evaluating surgical and medical devices related to renal calculus disease

Due to the structural and functional similarities between porcine and human kidneys, porcine models are widely used for translational evaluation of urolithiasis-related surgical techniques and medical devices. This review and Table 5 summarize representative porcine surgical device models, with emphasis on their typical applications and the translational questions that each model can or cannot address. Representative burst wave lithotripsy (BWL) studies

Table 5 Summary of CaOx stone models in pigs

Method	Diet/Intervention	Effects/Application	References
Exogenous induction	10% HLP for 1–5 days 15% HLP for 6–13 days 20% HLP for 14–21 days	Hyperoxaluria Collecting duct crystal deposition CaOx encrustation at renal papillary tips	Mandel et al., 2004
	10% HLP for 3–5 days	Hyperoxaluria	Kaplon et al., 2010
	5% HLP for 21–42 days	Collecting duct intraluminal crystal deposition	Sivalingam et al., 2013
	0.8% EG+2 μg/kg VD for 28 days 0.8% EG+AC 100 mg/kg 0.8% EG+G 5 mg/kg	Crystallization within renal cortex Renal medullary crystalline deposition nephrotoxicity	Trojan et al., 2017
Dietary manipulation	5%–10% HLP	Persistent hyperoxaluria Collecting duct intraluminal crystal deposition	Penniston et al., 2017
	Gelatin diet (containing 12% HLP)	Delayed-onset hyperoxaluria	
	High oxalate+low calcium diet (0.5 mg/mg)	Severe enteric hyperoxaluria	
	Normal oxalate+low calcium diet (3.6 mg/mg)	Mild hyperoxaluria Crystallization within renal cortex	
Surgery	Implantation of human COM stones into pig kidneys	BWL	Maxwell et al., 2019; Shelton et al., 2025; Wang et al., 2018
		Ultrasound propulsion	Bailey et al., 2018; Harper et al., 2013, 2014; Sorensen et al., 2010, 2013
		Ureteroscopy procedures	Chen et al., 2022b, 2022c; Deininger et al., 2018; Jiang et al., 2023; Molina et al., 2021; Oratis et al., 2018; Yang et al., 2024
		PCNL	Klein et al., 2018; O'Connor et al., 2022; Wakileh et al., 2024

AC: NH_4Cl, BWL: burst wave lithotripsy, CaOx: calcium oxalate, COM: calcium oxalate monohydrate, EG: ethylene glycol, G: gentamicin, HLP: hydroxyproline, KO: knockout, NaOx: sodium oxalate, PCNL: percutaneous nephrolithotomy, VD: Vitamin D.

use surgically implanted human stones to quantify lithotripsy efficacy and monitor renal safety under clinically relevant imaging and anesthesia conditions (Harper et al., 2013, 2014; Maxwell et al., 2019; Shelton et al., 2025; Sorensen et al., 2010; Wang et al., 2018). Ultrasound propulsion models utilize COM stones placed within the collecting system to evaluate noninvasive stone repositioning, removal, and potential safety at the ureteropelvic junction (Bailey et al., 2018; Chen et al., 2022b; Oratis et al., 2018; Yang et al., 2024). Porcine ureteroscopy models support training and direct comparison of access sheaths, endoscopes, stone baskets, and laser lithotripsy platforms, enabling assessment of maneuverability, irrigation pressure control, and procedure-related injury within a collecting system of human-like dimensions (Chen et al., 2022c; Deininger et al., 2018; Jiang et al., 2023; O'Connor et al., 2022; Molina et al., 2021; Wakileh et al., 2024). For endoscopic lithotripsy, the holmium:yttrium-aluminum-garnet (Ho:YAG) laser remains the dominant clinical device, whereas newer thulium fiber laser (TFL) platforms are gaining increasing attention in porcine models to compare pulverization or fragmentation efficacy and thermal safety under controlled irrigation conditions (Chen et al., 2022c; Deininger et al., 2018; Jiang et al., 2023; Molina et al., 2021; O'Connor et al., 2022; Wakileh et al., 2024). *In vivo* pig models and *ex vivo* porcine kidney models for percutaneous nephrolithotomy provide realistic puncture feedback and allow evaluation of puncture techniques, catheter dilation instruments, and safety performance (Alford et al., 2020; Chaussy et al., 1977, 1980; Klein et al., 2018; Mohamaden et al., 2014; Sorensen et al., 2013).

Prospects

Pig models have substantial value for validating surgical techniques and evaluating urolithiasis-related medical devices because porcine kidneys closely approximate human kidneys in anatomy and operative handling. However, high maintenance costs, specialized housing requirements, and technically demanding surgical modeling procedures continue to limit their widespread application.

CANINE MODELS

Artificial animal models

Canine stone models have contributed to the development and validation of surgical technologies. Chaussy et al. (1977) successfully established an artificial canine stone model by surgically implanting human calculi into dog kidneys. This model was subsequently used to demonstrate that extracorporeal shock wave lithotripsy could fragment stones effectively while producing fewer complications than conventional surgery (Chaussy et al., 1980).

Mohamaden et al. (2014) generated a chemically induced canine CaOx model using intravenous KOx, which produced crystal deposition and tubular dilatation in both the renal cortex and medulla. Notably, OPN mRNA expression increased 9.64-fold in the cortex and 12.72-fold in the medulla, whereas THP mRNA expression decreased 13.9-fold and 10.37-fold in the corresponding regions, respectively (Mohamaden et al., 2014). These findings indicate that OPN and THP participate in the renal response to oxalate exposure and suggest that KOx can be used to induce CaOx crystal-associated renal injury in dogs.Despite these applications, experimentally induced canine CaOx models remain uncommon. Ethical concerns are especially prominent for dogs because of their status as companion animals, which limits their routine use in invasive stone-modeling studies.

Naturally occurring animal models

Although dogs are rarely used in induced CaOx stone experiments, naturally occurring canine urolithiasis provides a valuable comparative model because dogs share human living environments, dietary exposures, and lifestyle-related risk factors. This naturally occurring model may help identify environmental and behavioral contributors to stone risk while avoiding some limitations of rapidly induced laboratory models, thereby offering a closer approximation of the spontaneous course of human stone disease (Alford et al., 2020).

Naturally occurring CaOx stone models: CaOx stones are among the most common forms of canine urolithiasis, accounting for approximately 38% of cases, with incidence showing a persistent upward trend (Osborne et al., 2009). Canine CaOx stone disease shows marked breed susceptibility, consistent with a strong genetic component; this parallels the 46%–63% heritability estimated for kidney stone disease in humans (Curhan et al., 1997; Goldfarb et al., 2005, 2019; Hemminki et al., 2018; Lekcharoensuk et al., 2000b; Low et al., 2010; Resnick et al., 1968). Additional risk factors include age, male sex, and obesity (Kennedy et al., 2016; Lekcharoensuk et al., 2000b; Low et al., 2010; Lulich et al., 1999). Idiopathic hypercalciuria is the most common urinary abnormality in dogs with CaOx stones, with a reported prevalence of 35%–65%, comparable to that observed in human patients (Carr et al., 2020; Dijcker et al., 2012; Furrow et al., 2015). Impaired vitamin D 24-hydroxylation can increase active vitamin D levels, enhance intestinal calcium absorption, and promote hypercalciuria, a mechanism validated in human studies (Groth et al., 2019; Ketha et al., 2015; Molin et al., 2015). In contrast, hyperoxaluria plays a relatively minor role in canine CaOx stone formation, as most affected dogs show renal oxalate excretion within the normal range or below that of unaffected dogs (Carvalho et al., 2006; Furrow et al., 2015; Lulich et al., 1991). Primary hyperoxaluria has been reported occasionally in certain breeds, but it typically manifests as renal tubular injury with extensive oxalate crystal deposition rather than typical stone development (Danpure et al., 1991; Jansen & Arnesen, 1990; Vidgren et al., 2012). Healthy dogs also show higher intestinal colonization by *Oxalobacter formigenes* compared with affected dogs, suggesting a potential protective role of this oxalate-degrading bacterium, consistent with findings in human studies (Gnanandarajah et al., 2012; Kaufman et al., 2008).

Prospects

Naturally occurring canine CaOx stone disease offers an important comparative model that captures spontaneous stone development, environmental exposure, genetic susceptibility, hypercalciuria, and microbiome-associated risk more closely than many induced laboratory models. However, ethical constraints, companion-animal status, and practical limitations restrict experimental manipulation and reduce the frequency of canine use as a dedicated animal model.

CAT MODELS

Comparative proteomics of the CaOx kidney stone matrix in cats and humans

CaOx kidney stones are common, recurrent, and strongly influenced by interactions between mineral crystals and the organic stone matrix, yet the precise contribution of the matrix to stone formation remains incompletely defined (Coe et al., 1992; Khan & Kok, 2004; Worcester, 1996). The stone matrix consists predominantly of proteins but also contains lipids, nucleic acids, and various organic residues (Boyce & Garvey, 1956). Proteomic studies have shown that feline COM kidney stone matrices closely resemble human COM stone matrices, with enrichment of highly charged proteins, greater overall charge than urinary proteins, and strong conservation of anionic protein composition (Wesson et al., 2022, 2024). These matrix proteins likely influence stone development through protein-protein and protein-crystal interactions that regulate crystal adhesion, aggregation, and growth (Rimer et al., 2017; Viswanathan et al., 2011; Wesson et al., 2005). The high proteomic similarity between feline and human COM stone matrices supports the potential value of cats as a naturally occurring comparative model for human CaOx stone disease (Wesson et al., 2022, 2024).

Naturally occurring CaOx stone models in cats

Naturally occurring feline CaOx kidney stone disease provides a comparative model for examining epidemiological, metabolic, pathological, and microbial features of spontaneous stone formation.

Epidemiology: Similar to dogs, cats commonly develop CaOx urolithiasis. CaOx stones accounted for approximately 60% of cases in the 1990s (Osborne et al., 2009). Subsequent dietary adjustments reduced struvite lower urinary tract stones, followed by a gradual increase in CaOx stone prevalence (Cannon et al., 2007; Kopecny et al., 2021; Lekcharoensuk et al., 2000a, 2001, 2005; Osborne et al., 2009). Currently, approximately 98% of feline kidney stones are CaOx, a proportion higher than that reported in humans (70%–80%) (Kopecny et al., 2021; Kyles et al., 2005; Lieske et al., 2014; Singh et al., 2015). Major risk factors include age greater than 10 years, male sex (particularly neutered males), dehydration with low urine output, and acidic urine (Osborne et al., 1996; Thumchai et al., 1996). Several breeds, including Persian, Himalayan, Ragdoll, and Burmese cats, exhibit marked genetic predisposition (Lekcharoensuk et al., 2000a; Thumchai et al., 1996). More than 80% of cats diagnosed with ureteral stones develop azotemia, and 25%–40% present with bilateral obstruction (Kyles et al., 2005; Nesser et al., 2018). Chronic kidney disease (CKD), which is prevalent in geriatric cats, is associated with renal calculi, although causality remains unconfirmed (Brown et al., 2016; Cléroux et al., 2017).

Metabolism: Metabolic risk profiles in feline CaOx stone disease differ from those described in dogs, and available data on feline hypercalciuria remain limited (Dijcker et al., 2012; Lulich et al., 2004; Ross et al., 1999). In one small study, approximately one-third of cats with CaOx urolithiasis had idiopathic hypercalcemia, although the underlying source of hypercalcemia was not identified (Lulich et al., 2004). Overall, idiopathic hypercalcemia appears uncommon in the general feline population (Coady et al., 2019; Midkiff et al., 2000). Primary hyperoxaluria is also rare in cats, although vitamin B6 deficiency can induce hyperoxaluria (Gershoff et al., 1959; McKerrell et al., 1989).

Pathology: Calcifications resembling human Randall's plaques have been observed in the renal papillary interstitium of cats with spontaneous CaOx stones (O'Kell et al., 2017). Small-scale studies and case reports have also described interstitial fibrosis, glomerulosclerosis, tubular oxalate crystal deposition, and inflammation, often in animals with concurrent

CKD (Chakrabarti et al., 2013; Heiene et al., 2009; Ross et al., 2007). These findings suggest that naturally occurring feline CaOx stone disease may provide a useful model for studying papillary mineralization and Randall's plaque-associated mechanisms.

Microorganisms: Medical research over the past two decades has demonstrated an association between intestinal and urinary tract dysbiosis and CaOx stone development, but comparable work in cats remains limited (Jung et al., 2023; Miller et al., 2022; Yuan et al., 2023). Robust sampling protocols are needed to define the contribution of gut and urinary microbiota to feline CaOx nephrolithiasis. Joubran et al. reported that cats with kidney stones exhibit a distinct urinary microbiome, with greater richness and diversity than healthy cats (Joubran et al., 2024a). In a separate methodological study, Joubran et al. further showed that fecal sampling methods influence the characterization of feline gut microbiota, supporting the need for standardized sampling protocols in studies of feline CaOx nephrolithiasis (Joubran et al., 2024b).

Prospects

Cats and dogs are mammalian companion animals that share human living environments and develop spontaneous CaOx stone disease with clinically relevant metabolic, pathological, and microbial features. Compared with artificially induced rodent models, these naturally occurring models more closely reflect the gradual development of human stone disease and may help identify environmental, genetic, dietary, and microbiome-associated risk factors. However, feline CaOx stone research remains limited.

CLINICAL TRANSLATION

Animal models have identified many candidate interventions with activity against CaOx stone formation, but only a few have progressed to human trials. This translational gap reflects limited concordance between experimental models and the natural progression of human disease, as well as inconsistent definitions of stone-specific endpoints. For example, hydroxycitric acid has been studied as an adjunct to extracorporeal shock wave lithotripsy in randomized, double-blind, placebo-controlled trials involving patients with CaOx stones, with stone fragmentation rate used as the primary endpoint (Del Carmen Cano García et al., 2023). Concurrently, microbiome-based oxalate management is advancing toward clinical evaluation. In a controlled dietary proof-of-concept study in healthy adults, ingestion of live *Oxalobacter formigenes* established sustained colonization and reduced urinary oxalate excretion (Fargue et al., 2025).

CONCLUSION

No animal model fully reproduces human CaOx stone disease. The most widely used models remain chemically induced rodent systems driven by short-term hyperoxaluria, which primarily reproduce intratubular crystallization and renal injury rather than the slow evolution of idiopathic human CaOx nephrolithiasis or the natural plaque-to-stone transformation. Model selection should therefore begin with a clearly defined human etiology and papillary mechanism, including idiopathic, primary hyperoxaluric, or enteric hyperoxaluric disease, as well as plaque- or plug-associated lithogenesis. Anticipated endpoints should also be specified in advance, including crystal burden, plaque formation, stone growth, stone expulsion, device performance, toxicity, and model failure modes.

This review proposes the first stepwise framework for CaOx stone model selection. *Drosophila* models are suited to high-throughput, low-cost screening of candidate pathways and therapeutic compounds. Rodent models provide the next level of mechanistic validation and safety assessment when matched to relevant etiologies, including primary or enteric hyperoxaluria, or plaque-associated processes such as Abcc6 deficiency. Large-animal and naturally occurring models, including pigs, dogs, and cats, then support evaluation of surgical device handling, complex renal physiology, spontaneous disease progression, and clinically relevant environmental or metabolic risk factors. Although preclinical studies have identified many promising anti-crystallization and anti-inflammatory candidates, few have advanced to rigorous human trials, likely because of persistent model-disease mismatch and non-standardized endpoint definitions. Future model development should therefore incorporate patient-derived data more directly. Recent single-cell RNA sequencing of human kidney tissue has begun to define cell-type-specific responses to Randall's plaque-associated injury, offering a path toward more precise characterization of idiopathic CaOx stone disease and the mechanisms underlying Randall's body formation (Iqbal et al., 2026).

COMPETING INTERESTS

The authors declare that they have no competing interests.

AUTHORS' CONTRIBUTIONS

X.T. and X.J. conceived and designed this study. X.T. drafted the manuscript. J.W., L.X., S.F., K.W. and C.C. revised the manuscript. All authors read and approved the final version of the manuscript.

REFERENCES

Ahsan SK, Tabiq M, Ageel AM, et al. 1989. Effect of *Trigonella foenum-graecum* and *ammi* majus on calcium oxalate urolithiasis in rats. *Journal of Ethnopharmacology*, **26**(3): 249–254.

Akouris PP, Chmiel JA, Stuivenberg GA, et al. 2023. Osteopontin phosphopeptide mitigates calcium oxalate stone formation in a *Drosophila melanogaster* model. *Urolithiasis*, **51**(1): 19.

Al KF, Daisley BA, Chanyi RM, et al. 2020. Oxalate-degrading *Bacillus subtilis* mitigates urolithiasis in a *Drosophila melanogaster* model. *mSphere*, **5**(5): e00498–20.

Alexander RT, Fuster DG, Dimke H. 2022. Mechanisms underlying calcium nephrolithiasis. *Annual Review of Physiology*, **84**: 559–583.

Alford A, Furrow E, Borofsky M, et al. 2020. Animal models of naturally occurring stone disease. *Nature Reviews Urology*, **17**(12): 691–705.

Amanzadeh J, Gitomer WL, Zerwekh JE, et al. 2003. Effect of high protein diet on stone-forming propensity and bone loss in rats. *Kidney International*, **64**(6): 2142–2149.

Amiel T, Srinivasan S, Turrina C, et al. 2025. Harnessing magnetism: evaluation of safety, tolerance and feasibility of magnetic kidney stone retrieval in vivo in porcine models. *Urolithiasis*, **53**(1): 12.

An LY, Li SJ, Chang ZL, et al. 2025. Gut microbiota modulation via fecal microbiota transplantation mitigates hyperoxaluria and calcium oxalate crystal depositions induced by high oxalate diet. *Gut Microbes*, **17**(1): 2457490.

Bagetti Filho HJS, Pereira-Sampaio MA, Favorito LA, et al. 2008. Pig kidney: anatomical relationships between the renal venous arrangement and the kidney collecting system. *The Journal of Urology*, **179**(4): 1627–1630.

Bailey MR, Wang YN, Kreider W, et al. 2018. Update on clinical trials of

kidney stone repositioning and preclinical results of stone breaking with one system. *Proceedings of Meetings on Acoustics*, **35**(1): 020004.

Bankir L, Figueres L, Prot-Bertoye C, et al. 2020. Medullary and cortical thick ascending limb: similarities and differences. *American Journal of Physiology-Renal Physiology*, **318**(2): F422–F442.

Blood FR. 1965. Chronic toxicity of ethylene glycol in the rat. *Food and Cosmetics Toxicology*, **3**: 229–234.

Bouderlique E, Tang E, Perez J, et al. 2019. Vitamin D and calcium supplementation accelerates Randall's plaque formation in a murine model. *The American Journal of Pathology*, **189**(11): 2171–2180.

Boyce WH, Garvey FK. 1956. The amount and nature of the organic matrix in urinary calculi: a review. *The Journal of Urology*, **76**(3): 213–227.

Brown CA, Elliott J, Schmiedt CW, et al. 2016. Chronic kidney disease in aged cats: clinical features, morphology, and proposed pathogeneses. *Veterinary Pathology*, **53**(2): 309–326.

Buchalski B, Wood KD, Challa A, et al. 2020. The effects of the inactivation of hydroxyproline dehydrogenase on urinary oxalate and glycolate excretion in mouse models of primary hyperoxaluria. *Biochimica et Biophysica Acta (BBA)-Molecular Basis of Disease*, **1866**(3): 165633.

Bushinsky DA, Asplin JR, Grynpas MD, et al. 2002. Calcium oxalate stone formation in genetic hypercalciuric stone-forming rats. *Kidney International*, **61**(3): 975–987.

Bushinsky DA, Favus MJ. 1988. Mechanism of hypercalciuria in genetic hypercalciuric rats. inherited defect in intestinal calcium transport. *The Journal of Clinical Investigation*, **82**(5): 1585–1591.

Bushinsky DA, Grynpas MD, Nilsson EL, et al. 1995. Stone formation in genetic hypercalciuric rats. *Kidney International*, **48**(6): 1705–1713.

Cannon AB, Westropp JL, Ruby AL, et al. 2007. Evaluation of trends in urolith composition in cats: 5, 230 cases (1985–2004). *Journal of the American Veterinary Medical Association*, **231**(4): 570–576.

Carr SV, Grant DC, DeMonaco SM, et al. 2020. Measurement of preprandial and postprandial urine calcium to creatinine ratios in male Miniature Schnauzers with and without urolithiasis. *Journal of Veterinary Internal Medicine*, **34**(2): 754–760.

Carvalho M, Lulich JP, Osborne CA, et al. 2006. Defective urinary crystallization inhibition and urinary stone formation. *International Braz J Urol : Official Journal of the Brazilian Society of Urology*, **32**(3): 342–348.

Chakrabarti S, Syme HM, Brown CA, et al. 2013. Histomorphometry of feline chronic kidney disease and correlation with markers of renal dysfunction. *Veterinary Pathology*, **50**(1): 147–155.

Chaussy C, Eisenberger F, Wanner K. 1977. The implantation of human kidney stones--a simple experimental model (author's transl). *Urologe A*, **16**(1): 35–38.

Chaussy CH, Brendel W, Schmiedt E. 1980. Extracorporeally induced destruction of kidney stones by shock waves. *The Lancet*, **316**(8207): 1265–1268.

Chen SJ, Dalanbaatar S, Chen HY, et al. 2022a. Astragalus membranaceus extract prevents calcium oxalate crystallization and extends lifespan in a *Drosophila urolithiasis* model. *Life*, **12**(8): 1250.

Chen WC, Wu HC, Lin WC, et al. 2001. The association of androgen- and oestrogen-receptor gene polymorphisms with urolithiasis in men. *BJU International*, **88**(4): 432–436.

Chen XW, Gu LQ, Zeng XY, et al. 2025. Sulfated *Pelvetia siliquosa* polysaccharides inhibit caox stone formation by inhibiting calcium oxalate crystallization, cellular inflammation, and crystal adhesion. *Journal of Agricultural and Food Chemistry*, **73**(2): 1542–1562.

Chen YH, Liu HP, Chen HY, et al. 2011. Ethylene glycol induces calcium oxalate crystal deposition in malpighian tubules: a drosophila model for nephrolithiasis/urolithiasis. *Kidney International*, **80**(4): 369–377.

Chen YJ, Li C, Gao L, et al. 2022c. Novel flexible vacuum-assisted ureteral access sheath can actively control intrarenal pressure and obtain a complete stone-free status. *Journal of Endourology*, **36**(9): 1143–1148.

Chen YJ, Liu W, Xi HB, et al. 2022b. The assistant effects of porcine fibrin sealant in improving stone clearance rate in flexible ureteroscopy lithotripsy in ex vivo porcine kidney model. *National Medical Journal of China*, **102**(22): 1660–1665. (in Chinese)

Cherng JH, Hsu YJ, Liu CC, et al. 2019. Activities of Ca^{2+}-related ion channels during the formation of kidney stones in an infection-induced urolithiasis rat model. *American Journal of Physiology-Renal Physiology*, **317**(5): F1342–F1349.

Chung J, Granja I, Taylor MG, et al. 2016. Molecular modifiers reveal a mechanism of pathological crystal growth inhibition. *Nature*, **536**(7617): 446–450.

Cil O, Chu T, Lee S, et al. 2022. Small-molecule inhibitor of intestinal anion exchanger SLC26A3 for treatment of hyperoxaluria and nephrolithiasis. *JCI Insight*, **7**(13): e153359.

Cléroux A, Alexander K, Beauchamp G, et al. 2017. Evaluation for association between urolithiasis and chronic kidney disease in cats. *Journal of the American Veterinary Medical Association*, **250**(7): 770–774.

Coady M, Fletcher DJ, Goggs R. 2019. Severity of ionized hypercalcemia and hypocalcemia is associated with etiology in dogs and cats. *Frontiers in Veterinary Science*, **6**: 276.

Coe FL, Parks JH, Asplin JR. 1992. The pathogenesis and treatment of kidney stones. *The New England Journal of Medicine*, **327**(16): 1141–1152.

Cohen E, Sawyer JK, Peterson NG, et al. 2020. Physiology, development, and disease modeling in the *Drosophila* excretory system. *Genetics*, **214**(2): 235–264.

Curhan GC, Willett WC, Rimm EB, et al. 1997. Family history and risk of kidney stones. *Journal of the American Society of Nephrology: JASN*, **8**(10): 1568–1573.

Danpure CJ, Jennings PR, Jansen JH. 1991. Enxymological characterization of a putative canine analogue of primary hyperoxaluria type 1. *Biochimica et Biophysica Acta (BBA) - Molecular Basis of Disease*, **1096**(2): 134–138.

Daudon M, Bazin D, Letavernier E. 2015. Randall's plaque as the origin of calcium oxalate kidney stones. *Urolithiasis*, **43 Suppl 1**: 5–11.

Dawson PA, Russell CS, Lee S, et al. 2010. Urolithiasis and hepatotoxicity are linked to the anion transporter sat1 in mice. *The Journal of Clinical Investigation*, **120**(3): 706–712.

de Water R, Boevé ER, van Miert PP, et al. 1996. Experimental nephrolithiasis in rats: the effect of ethylene glycol and vitamin d3 on the induction of renal calcium oxalate crystals. *Scanning Microscopy*, **10**(2): 591–601.

De Yoreo JJ, Qiu SR, Hoyer JR. 2006. Molecular modulation of calcium oxalate crystallization. *American Journal of Physiology-Renal Physiology*, **291**(6): F1123–F1132.

Deguchi R, Komori T, Yamashita S, et al. 2024. Suppression of renal crystal formation, inflammation, and fibrosis by blocking oncostatin m receptor β signaling. *Scientific Reports*, **14**(1): 28913.

Deininger S, Haberstock L, Kruck S, et al. 2018. Single-use versus reusable ureterorenoscopes for retrograde intrarenal surgery (RIRS): systematic comparative analysis of physical and optical properties in three different devices. *World Journal of Urology*, **36**(12): 2059–2063.

Del Carmen Cano García M, Cobos RC, Bohorquez ÁV, et al. 2023. A randomized, double-blind, placebo-controlled clinical trial of the use of hydroxycitric acid adjuvant to shock wave lithotripsy therapy in patients with calcium stones. Stone fragmentation results. *Urolithiasis*, **51**(1): 83.

Devuyst O, Dahan K, Pirson Y. 2005. Tamm-Horsfall protein or uromodulin: new ideas about an old molecule. *Nephrology Dialysis Transplantation*, **20**(7): 1290–1294.

Devuyst O, Olinger E, Rampoldi L. 2017. Uromodulin: from physiology to rare and complex kidney disorders. *Nature Reviews Nephrology*, **13**(9): 525–544.

Dijcker JC, Kummeling A, Hagen-Plantinga EA, et al. 2012. Urinary oxalate

and calcium excretion by dogs and cats diagnosed with calcium oxalate urolithiasis. *Veterinary Record*, **171**(25): 646.

Dong F, Jiang S, Tang C, et al. 2022. Trimethylamine N-oxide promotes hyperoxaluria-induced calcium oxalate deposition and kidney injury by activating autophagy. *Free Radical Biology and Medicine*, **179**: 288–300.

Dow JAT, Simons M, Romero MF. 2022. *Drosophila melanogaster*: a simple genetic model of kidney structure, function and disease. *Nature Reviews Nephrology*, **18**(7): 417–434.

Duscha A, Gisevius B, Hirschberg S, et al. 2020. Propionic acid shapes the multiple sclerosis disease course by an immunomodulatory mechanism. *Cell*, **180**(6): 1067–1080. e16.

Eder AF, McGrath CM, Dowdy YG, et al. 1998. Ethylene glycol poisoning: toxicokinetic and analytical factors affecting laboratory diagnosis. *Clinical Chemistry*, **44**(1): 168–177.

Ermer T, Nazzal L, Tio MC, et al. 2023. Oxalate homeostasis. *Nature Reviews Nephrology*, **19**(2): 123–138.

Evan AP, Coe FL, Lingeman JE, et al. 2007. Mechanism of formation of human calcium oxalate renal stones on Randall's plaque. *The Anatomical Record*, **290**(10): 1315–1323.

Fachi JL, Sécca C, Rodrigues PB, et al. 2020. Acetate coordinates neutrophil and ILC3 responses against *C. difficile* through FFAR2. *Journal of Experimental Medicine*, **217**(3): e20190489.

Fan QX, Gong SQ, Hong XZ, et al. 2020. Clinical-grade *Garcinia cambogia* extract dissolves calcium oxalate crystals in *Drosophila* kidney stone models. *European Review for Medical and Pharmacological Sciences*, **24**(11): 6434–6445.

Fargue S, Suryavanshi M, Wood KD, et al. 2025. Inducing *Oxalobacter formigenes* colonization reduces urinary oxalate in healthy adults. *Kidney International Reports*, **10**(5): 1518–1528.

Farmanesh S, Ramamoorthy S, Chung J, et al. 2014. Specificity of growth inhibitors and their cooperative effects in calcium oxalate monohydrate crystallization. *Journal of the American Chemical Society*, **136**(1): 367–376.

Freel RW, Whittamore JM, Hatch M. 2013. Transcellular oxalate and Cl^- absorption in mouse intestine is mediated by the DRA anion exchanger Slc26a3, and DRA deletion decreases urinary oxalate. *American Journal of Physiology-Gastrointestinal and Liver Physiology*, **305**(7): G520–G527.

Furrow E, Patterson EE, Armstrong PJ, et al. 2015. Fasting urinary calcium-to-creatinine and oxalate-to-creatinine ratios in dogs with calcium oxalate urolithiasis and breed-matched controls. *Journal of Veterinary Internal Medicine*, **29**(1): 113–119.

GBD 2021 Urolithiasis Collaborators. 2024. The global, regional, and national burden of urolithiasis in 204 countries and territories, 2000–2021: a systematic analysis for the global burden of disease study 2021. *EClinicalMedicine*, **78**: 102924.

Gershoff SN, Faragalla FF, Nelson DA, et al. 1959. Vitamin B_6 deficiency and oxalate nephrocalcinosis in the cat. *The American Journal of Medicine*, **27**(1): 72–80.

Giachelli CM, Steitz S. 2000. Osteopontin: a versatile regulator of inflammation and biomineralization. *Matrix Biology*, **19**(7): 615–622.

Gnanandarajah JS, Abrahante JE, Lulich JP, et al. 2012. Presence of *Oxalobacter formigenes* in the intestinal tract is associated with the absence of calcium oxalate urolith formation in dogs. *Urological Research*, **40**(5): 467–473.

Golbaekdal K, Nielsen CB, Pedersen EB. 1996. The acute effects of FK-506 on renal haemodynamics, water and sodium excretion and plasma levels of angiotensin II, aldosterone, atrial natriuretic peptide and vasopressin in pigs. *Journal of Pharmacy and Pharmacology*, **48**(11): 1174–1179.

Goldfarb DS, Avery AR, Beara-Lasic L, et al. 2019. A twin study of genetic influences on nephrolithiasis in women and men. *Kidney International Reports*, **4**(4): 535–540.

Goldfarb DS, Fischer ME, Keich Y, et al. 2005. A twin study of genetic and dietary influences on nephrolithiasis: a report from the Vietnam era twin (VET) registry. *Kidney International*, **67**(3): 1053–1061.

Groth EM, Lulich JP, Chew DJ, et al. 2019. Vitamin d metabolism in dogs with and without hypercalciuric calcium oxalate urolithiasis. *Journal of Veterinary Internal Medicine*, **33**(2): 758–763.

Guertin DA, Sabatini DM. 2007. Defining the role of mTOR in cancer. *Cancer Cell*, **12**(1): 9–22.

Han ZY, Wang BS, Liu XH, et al. 2023. Intrarenal pressure study using 7.5 French flexible ureteroscope with or without ureteral access sheath in an ex-vivo porcine kidney model. *World Journal of Urology*, **41**(11): 3129–3134.

Hansen-Estruch C, Cooper DKC, Judd E. 2022. Physiological aspects of pig kidney xenotransplantation and implications for management following transplant. *Xenotransplantation*, **29**(3): e12743.

Hanstock S, Ferreira D, Adomat H, et al. 2025. A mouse model for the study of diet-induced changes in intestinal microbiome composition on renal calcium oxalate crystal formation. *Urolithiasis*, **53**(1): 4.

Harper JD, Dunmire B, Wang YN, et al. 2014. Preclinical safety and effectiveness studies of ultrasonic propulsion of kidney stones. *Urology*, **84**(2): 484–489.

Harper JD, Sorensen MD, Cunitz BW, et al. 2013. Focused ultrasound to expel calculi from the kidney: safety and efficacy of a clinical prototype device. *The Journal of Urology*, **190**(3): 1090–1095.

Heiene R, Rumsby G, Ziener M, et al. 2009. Chronic kidney disease with three cases of oxalate-like nephrosis in ragdoll cats. *Journal of Feline Medicine and Surgery*, **11**(6): 474–480.

Hemminki K, Hemminki O, Försti A, et al. 2018. Familial risks in urolithiasis in the population of sweden. *BJU International*, **121**(3): 479–485.

Hermanns HM. 2015. Oncostatin m and interleukin-31: cytokines, receptors, signal transduction and physiology. *Cytokine & Growth Factor Reviews*, **26**(5): 545–558.

Hoopes Jr RR, Reid R, Sen S, et al. 2003. Quantitative trait loci for hypercalciuria in a rat model of kidney stone disease. *Journal of the American Society of Nephrology*, **14**(7): 1844–1850.

Howles SA, Thakker RV. 2020. Genetics of kidney stone disease. *Nature Reviews Urology*, **17**(7): 407–421.

Huang JN, Bayliss G, Zhuang SG. 2021. Porcine models of acute kidney injury. *American Journal of Physiology-Renal Physiology*, **320**(6): F1030–F1044.

Huang YC, Liu CJ, Lu ZH, et al. 2024. Long-term sodium deficiency reduces sodium excretion but impairs renal function and increases stone formation in hyperoxaluric calcium oxalate rats. *International Journal of Molecular Sciences*, **25**(7): 3942.

Iqbal MS, Duan XL, Attia KA, et al. 2026. FABP3 deficiency exacerbates renal randall plaque formation: insights from single-cell RNA transcriptomic analysis. *Molecular and Cellular Biochemistry*, **481**(2): 959–979.

Jansen JH, Arnesen K. 1990. Oxalate nephropathy in a Tibetan spaniel litter. A probable case of primary hyperoxaluria. *Journal of Comparative Pathology*, **103**(1): 79–84.

Jiang PB, Okhunov Z, Afyouni AS, et al. 2023. Comparison of superpulse thulium fiber laser vs holmium laser for ablation of renal calculi in an in vivo porcine model. *Journal of Endourology*, **37**(3): 335–340.

Jiang ZR, Asplin JR, Evan AP, et al. 2006. Calcium oxalate urolithiasis in mice lacking anion transporter Slc26a6. *Nature Genetics*, **38**(4): 474–478.

Jin X, Jian ZY, Chen XT, et al. 2021. Short chain fatty acids prevent glyoxylate-induced calcium oxalate stones by GPR43-dependent immunomodulatory mechanism. *Frontiers in Immunology*, **12**: 729382.

Joubran P, Roux FA, Serino M, et al. 2024a. Gut and urinary microbiota in cats with kidney stones. *Microorganisms*, **12**(6): 1098.

Joubran P, Roux FA, Serino M, et al. 2024b. Gut microbiota comparison in rectal swabs versus stool samples in cats with kidney stones. *Microorganisms*, **12**(12): 2411.

Jung HD, Cho S, Lee JY. 2023. Update on the effect of the urinary microbiome on urolithiasis. *Diagnostics*, **13**(5): 951.

Kale MD, Kadam SP, Shravage BV, et al. 2024. From computational prediction to experimental validation: hesperidin's anti-urolithiatic activity in sodium oxalate-induced urolithiasis models in fruit flies and mice. *Toxicology and Applied Pharmacology*, **492**: 117104.

Kaplon DM, Penniston KL, Darriet C, et al. 2010. Second prize: hydroxyproline-induced hyperoxaluria using acidified and traditional diets in the porcine model. *Journal of Endourology*, **24**(3): 355–359.

Kaufman DW, Kelly JP, Curhan GC, et al. 2008. *Oxalobacter formigenes* may reduce the risk of calcium oxalate kidney stones. *Journal of the American Society of Nephrology*, **19**(6): 1197–1203.

Kennedy SM, Lulich JP, Ritt MG, et al. 2016. Comparison of body condition score and urinalysis variables between dogs with and without calcium oxalate uroliths. *Journal of the American Veterinary Medical Association*, **249**(11): 1274–1280.

Ketha H, Singh RJ, Grebe SK, et al. 2015. Altered calcium and vitamin d homeostasis in first-time calcium kidney stone-formers. *PLoS One*, **10**(9): e0137350.

Khan SR. 1997. Animal models of kidney stone formation: an analysis. *World Journal of Urology*, **15**(4): 236–243.

Khan SR. 2010. Nephrocalcinosis in animal models with and without stones. *Urological Research*, **38**(6): 429–438.

Khan SR, Canales BK, Dominguez-Gutierrez PR. 2021. Randall's plaque and calcium oxalate stone formation: role for immunity and inflammation. *Nature Reviews Nephrology*, **17**(6): 417–433.

Khan SR, Finlayson B, Hackett RL. 1979. Histologic study of the early events in oxalate induced intranephronic calculosis. *Investigative Urology*, **17**(3): 199–202.

Khan SR, Finlayson B, Hackett RL. 1982. Experimental calcium oxalate nephrolithiasis in the rat. Role of the renal papilla. *The American Journal of Pathology*, **107**(1): 59–69.

Khan SR, Finlayson B, Hackett RL. 1983. Experimental induction of crystalluria in rats using mini-osmotic pumps. *Urological Research*, **11**(5): 199–205.

Khan SR, Glenton PA. 2008. Calcium oxalate crystal deposition in kidneys of hypercalciuric mice with disrupted type IIa sodium-phosphate cotransporter. *American Journal of Physiology-Renal Physiology*, **294**(5): F1109–F1115.

Khan SR, Glenton PA. 2010. Experimental induction of calcium oxalate nephrolithiasis in mice. *The Journal of Urology*, **184**(3): 1189–1196.

Khan SR, Glenton PA, Byer KJ. 2006. Modeling of hyperoxaluric calcium oxalate nephrolithiasis: experimental induction of hyperoxaluria by hydroxy-L-proline. *Kidney International*, **70**(5): 914–923.

Khan SR, Kok DJ. 2004. Modulators of urinary stone formation. *Frontiers in Bioscience*, **9**: 1450–1482.

Khan SR, Pearle MS, Robertson WG, et al. 2016. Kidney stones. *Nature Reviews Disease Primers*, **2**: 16008.

Khan SR, Rodriguez DE, Gower LB, et al. 2012. Association of Randall plaque with collagen fibers and membrane vesicles. *The Journal of Urology*, **187**(3): 1094–1100.

Kim YJ, Lee JY, Yang MJ, et al. 2022. Therapeutic effect of intra-articular injected 3'-sialyllactose on a minipig model of rheumatoid arthritis induced by collagen. *Laboratory Animal Research*, **38**(1): 8.

Klein JT, Rassweiler J, Rassweiler-Seyfried MC. 2018. Validation of a novel cost effective easy to produce and durable *in vitro* model for kidney-puncture and percutaneous nephrolitholapaxy-simulation. *Journal of Endourology*, **32**(9): 871–876.

Knauf F, Preisig PA. 2011. *Drosophila*: a fruitful model for calcium oxalate nephrolithiasis?. *Kidney International*, **80**(4): 327–329.

Knight J, Holmes RP. 2005. Mitochondrial hydroxyproline metabolism: implications for primary hyperoxaluria. *American Journal of Nephrology*, **25**(2): 171–175.

Knight J, Holmes RP, Cramer SD, et al. 2012. Hydroxyproline metabolism in mouse models of primary hyperoxaluria. *American Journal of Physiology-Renal Physiology*, **302**(6): F688–F693.

Knight J, Jiang J, Assimos DG, et al. 2006. Hydroxyproline ingestion and urinary oxalate and glycolate excretion. *Kidney International*, **70**(11): 1929–1934.

Koh A, De Vadder F, Kovatcheva-Datchary P, et al. 2016. From dietary fiber to host physiology: short-chain fatty acids as key bacterial metabolites. *Cell*, **165**(6): 1332–1345.

Kok DJ, Boellaard W, Ridwan Y, et al. 2017. Timelines of the "free-particle" and "fixed-particle" models of stone-formation: theoretical and experimental investigations. *Urolithiasis*, **45**(1): 33–41.

Kopecny L, Palm CA, Segev G, et al. 2021. Urolithiasis in cats: evaluation of trends in urolith composition and risk factors (2005–2018). *Journal of Veterinary Internal Medicine*, **35**(3): 1397–1405.

Krieger NS, Asplin J, Granja I, et al. 2021. Chlorthalidone with potassium citrate decreases calcium oxalate stones and increases bone quality in genetic hypercalciuric stone-forming rats. *Kidney International*, **99**(5): 1118–1126.

Kwenda EP, Rabley AK, Canales BK. 2020. Lessons from rodent gastric bypass model of enteric hyperoxaluria. *Current Opinion in Nephrology and Hypertension*, **29**(4): 400–406.

Kyles AE, Hardie EM, Wooden BG, et al. 2005. Clinical, clinicopathologic, radiographic, and ultrasonographic abnormalities in cats with ureteral calculi: 163 cases (1984–2002). *Journal of the American Veterinary Medical Association*, **226**(6): 932–936.

Lan Y, Zhu W, Duan XL, et al. 2021. Glycine suppresses kidney calcium oxalate crystal depositions via regulating urinary excretions of oxalate and citrate. *Journal of Cellular Physiology*, **236**(10): 6824–6835.

Landry GM, Hirata T, Anderson JB, et al. 2016. Sulfate and thiosulfate inhibit oxalate transport via a dPrestin (Slc26a6)-dependent mechanism in an insect model of calcium oxalate nephrolithiasis. *American Journal of Physiology-Renal Physiology*, **310**(2): F152–F159.

Lavelle A, Sokol H. 2020. Gut microbiota-derived metabolites as key actors in inflammatory bowel disease. *Nature Reviews Gastroenterology & Hepatology*, **17**(4): 223–237.

Lee SC, Kim YJ, Kim TH, et al. 2008. Impact of obesity in patients with urolithiasis and its prognostic usefulness in stone recurrence. *The Journal of Urology*, **179**(2): 570–574.

Lekcharoensuk C, Lulich JP, Osborne CA, et al. 2000a. Association between patient-related factors and risk of calcium oxalate and magnesium ammonium phosphate urolithiasis in cats. *Journal of the American Veterinary Medical Association*, **217**(4): 520–525.

Lekcharoensuk C, Lulich JP, Osborne CA, et al. 2000b. Patient and environmental factors associated with calcium oxalate urolithiasis in dogs. *Journal of the American Veterinary Medical Association*, **217**(4): 515–519.

Lekcharoensuk C, Osborne CA, Lulich JP, et al. 2001. Association between dietary factors and calcium oxalate and magnesium ammonium phosphate urolithiasis in cats. *Journal of the American Veterinary Medical Association*, **219**(9): 1228–1237.

Lekcharoensuk C, Osborne CA, Lulich JP, et al. 2005. Trends in the frequency of calcium oxalate uroliths in the upper urinary tract of cats. *Journal of the American Animal Hospital Association*, **41**(1): 39–46.

Letavernier E, Bouderlique E, Zaworski J, et al. 2019. Pseudoxanthoma elasticum, kidney stones and pyrophosphate: from a rare disease to urolithiasis and vascular calcifications. *International Journal of Molecular Sciences*, **20**(24): 6353.

Letavernier E, Kauffenstein G, Huguet L, et al. 2018. ABCC6 deficiency promotes development of Randall plaque. *Journal of the American Society of Nephrology*, **29**(9): 2337–2347.

Letavernier E, Verrier C, Goussard F, et al. 2016. Calcium and vitamin d

have a synergistic role in a rat model of kidney stone disease. *Kidney International*, **90**(4): 809–817.

Li JY, Zhou T, Gao XF, et al. 2010. Testosterone and androgen receptor in human nephrolithiasis. *The Journal of Urology*, **184**(6): 2360–2363.

Li QL, Krieger NS, Yang L, et al. 2024. Magnesium decreases urine supersaturation but not calcium oxalate stone formation in genetic hypercalciuric stone-forming rats. *Nephron*, **148**(7): 480–486.

Liang L, Li L, Tian J, et al. 2014. Androgen receptor enhances kidney Stone-CaOx crystal formation via modulation of oxalate biosynthesis & oxidative stress. *Molecular Endocrinology*, **28**(8): 1291–1303.

Lieske JC, Rule AD, Krambeck AE, et al. 2014. Stone composition as a function of age and sex. *Clinical Journal of the American Society of Nephrology*, **9**(12): 2141–2146.

Liu CJ, Ho KT, Huang HS, et al. 2025. Sodium glucose co-transporter 2 inhibitor prevents nephrolithiasis in non-diabetes by restoring impaired autophagic flux. *EBioMedicine*, **114**: 105668.

Liu Y, Jin X, Hong HG, et al. 2020. The relationship between gut microbiota and short chain fatty acids in the renal calcium oxalate stones disease. *The FASEB Journal*, **34**(8): 11200–11214.

Liu Y, Jin X, Ma YC, et al. 2021a. Short-chain fatty acids reduced renal calcium oxalate stones by regulating the expression of intestinal oxalate transporter SLC26A6. *mSystems*, **6**(6): e01045–21.

Liu Y, Jin X, Tian L, et al. 2021b. *Lactiplantibacillus plantarum* reduced renal calcium oxalate stones by regulating arginine metabolism in gut microbiota. *Frontiers in Microbiology*, **12**: 743097.

Low WW, Uhl JM, Kass PH, et al. 2010. Evaluation of trends in urolith composition and characteristics of dogs with urolithiasis: 25, 499 cases (1985–2006). *Journal of the American Veterinary Medical Association*, **236**(2): 193–200.

Lu Y, Wu ZL, Du ZX, et al. 2024. The anti-urolithiasis activity and safety of strangury-relieving herbs: a comparative study based on fruit fly kidney stone model. *Journal of Ethnopharmacology*, **326**: 117968.

Lulich JP, Osborne CA, Lekcharoensuk C, et al. 2004. Effects of diet on urine composition of cats with calcium oxalate urolithiasis. *Journal of the American Animal Hospital Association*, **40**(3): 185–191.

Lulich JP, Osborne CA, Nagode LA, et al. 1991. Evaluation of urine and serum metabolites in miniature schnauzers with calcium oxalate urolithiasis. *American Journal of Veterinary Research*, **52**(10): 1583–1590.

Lulich JP, Osborne CA, Thumchai R, et al. 1999. Epidemiology of canine calcium oxalate uroliths: identifying risk factors. *Veterinary Clinics of North America: Small Animal Practice*, **29**(1): 113–122.

Lyon ES, Borden TA, Vermeulen CW. 1966. Experimental oxalate lithiasis produced with ethylene glycol. *Investigative Urology*, **4**(2): 143–151.

Ma WC, Lutsko JF, Rimer JD, et al. 2020. Antagonistic cooperativity between crystal growth modifiers. *Nature*, **577**(7791): 497–501.

Mandel NS, Henderson JD, Hung LY, et al. 2004. A porcine model of calcium oxalate kidney stone disease. *The Journal of Urology*, **171**(3): 1301–1303.

Maxwell AD, Wang YN, Kreider W, et al. 2019. Evaluation of renal stone comminution and injury by burst wave lithotripsy in a pig model. *Journal of Endourology*, **33**(10): 787–792.

McKerrell RE, Blakemore WF, Heath MF, et al. 1989. Primary hyperoxaluria (L-glyceric aciduria) in the cat: a newly recognised inherited disease. *The Veterinary Record*, **125**(2): 31–34.

Meneton P, Ichikawa I, Inagami T, et al. 2000. Renal physiology of the mouse. *American Journal of Physiology-Renal Physiology*, **278**(3): F339–F351.

Midkiff AM, Chew DJ, Randolph JF, et al. 2000. Idiopathic hypercalcemia in cats. *Journal of Veterinary Internal Medicine*, **14**(6): 619–626.

Miller AW, Penniston KL, Fitzpatrick K, et al. 2022. Mechanisms of the intestinal and urinary microbiome in kidney stone disease. *Nature Reviews Urology*, **19**(12): 695–707.

Miller J, Chi T, Kapahi P, et al. 2013. Drosophila melanogaster as an emerging translational model of human nephrolithiasis. *The Journal of Urology*, **190**(5): 1648–1656.

Mo L, Huang HY, Zhu XH, et al. 2004. Tamm-Horsfall protein is a critical renal defense factor protecting against calcium oxalate crystal formation. *Kidney International*, **66**(3): 1159–1166.

Mo L, Liaw L, Evan AP, et al. 2007. Renal calcinosis and stone formation in mice lacking osteopontin, Tamm-Horsfall protein, or both. *American Journal of Physiology-Renal Physiology*, **293**(6): F1935–F1943.

Mohamaden W, Wang H, Guan HW, et al. 2014. Immunohistochemical localization and mRNA quantification of osteopontin and Tamm-Horsfall protein in canine renal tissue after potassium oxalate injection. *BMC Veterinary Research*, **10**(1): 70.

Molin A, Baudoin R, Kaufmann M, et al. 2015. *CYP24A1* mutations in a cohort of hypercalcemic patients: evidence for a recessive trait. *The Journal of Clinical Endocrinology & Metabolism*, **100**(10): E1343–E1352.

Molina WR, Carrera RV, Chew BH, et al. 2021. Temperature rise during ureteral laser lithotripsy: comparison of super pulse thulium fiber laser (SPTF) vs high power 120 W holmium-YAG laser (HO: YAG). *World Journal of Urology*, **39**(10): 3951–3956.

Naghii MR, Babaei M, Hedayati M. 2014. Androgens involvement in the pathogenesis of renal stones formation. *PLoS One*, **9**(4): e93790.

Nanamatsu A, de Araújo L, LaFavers KA, et al. 2024. Advances in uromodulin biology and potential clinical applications. *Nature Reviews Nephrology*, **20**(12): 806–821.

Nesser VE, Reetz JA, Clarke DL, et al. 2018. Radiographic distribution of ureteral stones in 78 cats. *Veterinary Surgery*, **47**(7): 895–901.

Nicholson TB, Chen TP, Richard S. 2009. The physiological and pathophysiological role of PRMT1-mediated protein arginine methylation. *Pharmacological Research*, **60**(6): 466–474.

O'Connor CJ, Hogan D, Yap LC, et al. 2022. An ex-vivo assessment of a new single probe triple modality (trilogy) lithotripter. *World Journal of Urology*, **40**(10): 2561–2566.

O'Kell AL, Grant DC, Khan SR. 2017. Pathogenesis of calcium oxalate urinary stone disease: species comparison of humans, dogs, and cats. *Urolithiasis*, **45**(4): 329–336.

Ogawa Y, Yamaguchi K, Morozumi M. 1990. Effects of magnesium salts in preventing experimental oxalate urolithiasis in rats. *The Journal of Urology*, **144**(2 Pt 1): 385–389.

Ogawa Y, Yamaguchi K, Tanaka T, et al. 1986. Effects of pyruvate salts, pyruvic acid, and bicarbonate salts in preventing experimental oxalate urolithiasis in rats. *The Journal of Urology*, **135**(5): 1057–1060.

Okada A, Nomura S, Higashibata Y, et al. 2007. Successful formation of calcium oxalate crystal deposition in mouse kidney by intraabdominal glyoxylate injection. *Urological Research*, **35**(2): 89–99.

Oratis AT, Subasic JJ, Hernandez N, et al. 2018. A simple fluid dynamic model of renal pelvis pressures during ureteroscopic kidney stone treatment. *PLoS One*, **13**(11): e0208209.

Osborne CA, Lulich JP, Kruger JM, et al. 2009. Analysis of 451, 891 canine uroliths, feline uroliths, and feline urethral plugs from 1981 to 2007: perspectives from the minnesota urolith center. *Veterinary Clinics of North America: Small Animal Practice*, **39**(1): 183–197.

Osborne CA, Lulich JP, Thumchai R, et al. 1996. Feline urolithiasis: etiology and pathophysiology. *Veterinary Clinics of North America: Small Animal Practice*, **26**(2): 217–232.

Patel SR, Penniston KL, Iwicki L, et al. 2012. Dietary induction of long-term hyperoxaluria in the porcine model. *Journal of Endourology*, **26**(5): 433–438.

Peerapen P, Thongboonkerd V. 2023. Kidney stone prevention. *Advances in Nutrition*, **14**(3): 555–569.

Penniston KL, Patel SR, Schwahn DJ, et al. 2017. Studies using a porcine model: what insights into human calcium oxalate stone formation

mechanisms has this model facilitated?. *Urolithiasis*, **45**(1): 109–125.

Pique C, Marsden E, Quesada P, et al. 2018. A shortened study design for embryo-fetal development studies in the minipig. *Reproductive Toxicology*, **80**: 35–43.

Randall A. 1936. An hypothesis for the origin of renal calculus. *The New England Journal of Medicine*, **214**(6): 234–242.

Rassweiler-Seyfried MC, Mayer J, Goldenstedt C, et al. 2023. High-frequency shock wave lithotripsy: stone comminution and evaluation of renal parenchyma injury in a porcine ex-vivo model. *World Journal of Urology*, **41**(7): 1929–1934.

Ren Y, Cui SY, Hong Q, et al. 2022. Role of nod-like receptors in a miniature pig model of diabetic renal injuries. *Mediators of Inflammation*, **2022**: 5515305.

Ren YN, Zhang W, Li YX, et al. 2025. Streamlined strategy for discovering active compounds for nephrolithiasis treatment from herbal medicines using the fruit fly model. *Journal of Ethnopharmacology*, **348**: 119846.

Renner S, Blutke A, Clauss S, et al. 2020. Porcine models for studying complications and organ crosstalk in diabetes mellitus. *Cell and Tissue Research*, **380**(2): 341–378.

Resnick M, Pridgen DB, Goodman HO. 1968. Genetic predisposition to formation of calcium oxalate renal calculi. *The New England Journal of Medicine*, **278**(24): 1313–1318.

Reynolds CJ, Turin DR, Romero MF. 2021. Transporters and tubule crystals in the insect Malpighian tubule. *Current Opinion in Insect Science*, **47**: 82–89.

Rimer JD, An ZH, Zhu Z, et al. 2010. Crystal growth inhibitors for the prevention of l-cystine kidney stones through molecular design. *Science*, **330**(6002): 337–341.

Rimer JD, Kolbach-Mandel AM, Ward MD, et al. 2017. The role of macromolecules in the formation of kidney stones. *Urolithiasis*, **45**(1): 57–74.

Ross SJ, Osborne CA, Lekcharoensuk C, et al. 2007. A case-control study of the effects of nephrolithiasis in cats with chronic kidney disease. *Journal of the American Veterinary Medical Association*, **230**(12): 1854–1859.

Ross SJ, Osborne CA, Lulich JP, et al. 1999. Canine and feline nephrolithiasis: epidemiology, detection, and management. *Veterinary Clinics of North America: Small Animal Practice*, **29**(1): 231–250.

Rossano AJ, Zhang LL, Anderson JB, et al. 2025. *Ex vivo* quantification of intracellular pH in *drosophila* malpighian tubule reveals basolateral HCO_3^-/oxalate exchange through a novel oxalate transporter “neat”. *Frontiers in Physiology*, **16**: 1468451.

Roth JA, Tuggle CK. 2015. Livestock models in translational medicine. *ILAR Journal*, **56**(1): 1–6.

Runyan TJ, Gershoff SN. 1965. The effect of vitamin B_6 deficiency in rats on the metabolism of oxalic acid precursors. *Journal of Biological Chemistry*, **240**(5): 1889–1892.

Salido EC, Li XM, Lu Y, et al. 2006. Alanine-glyoxylate aminotransferase-deficient mice, a model for primary hyperoxaluria that responds to adenoviral gene transfer. *Proceedings of the National Academy of Sciences of the United States of America*, **103**(48): 18249–18254.

Sampaio FJ, Pereira-Sampaio MA, Favorito LA. 1998. The pig kidney as an endourologic model: anatomic contribution. *Journal of Endourology*, **12**(1): 45–50.

Serafini-Cessi F, Malagolini N, Cavallone D. 2003. Tamm-Horsfall glycoprotein: biology and clinical relevance. *American Journal of Kidney Diseases*, **42**(4): 658–676.

Shelton TM, Connors BA, Rivera ME, et al. 2025. No injury observed in kidneys treated with burst wave lithotripsy in therapeutically anticoagulated pigs. *Journal of Endourology*, **39**(8): 804–807.

Singh P, Enders FT, Vaughan LE, et al. 2015. Stone composition among first-time symptomatic kidney stone formers in the community. *Mayo Clinic Proceedings*, **90**(10): 1356–1365.

Singh P, Harris PC, Sas DJ, et al. 2022. The genetics of kidney stone disease and nephrocalcinosis. *Nature Reviews Nephrology*, **18**(4): 224–240.

Sivalingam S, Nakada SY, Sehgal PD, et al. 2013. Dietary hydroxyproline induced calcium oxalate lithiasis and associated renal injury in the porcine model. *Journal of Endourology*, **27**(12): 1493–1498.

Song QL, Song C, Chen X, et al. 2023. FKBP5 deficiency attenuates calcium oxalate kidney stone formation by suppressing cell-crystal adhesion, apoptosis and macrophage m1 polarization via inhibition of NF-κB signaling. *Cellular and Molecular Life Sciences*, **80**(10): 301.

Sorensen MD, Bailey MR, Hsi RS, et al. 2013. Focused ultrasonic propulsion of kidney stones: review and update of preclinical technology. *Journal of Endourology*, **27**(10): 1183–1186.

Sorensen MD, Shah AR, Canney MS, et al. 2010. Ureteroscopic ultrasound technology to size kidney stone fragments: proof of principle using a miniaturized probe in a porcine model. *Journal of Endourology*, **24**(6): 939–942.

Su MJ, Sang SY, Liang TT, et al. 2023. PPARG: a novel target for yellow tea in kidney stone prevention. *International Journal of Molecular Sciences*, **24**(15): 11955.

Su XZ, Chen HB, Xiang H, et al. 2024a. Selenium participates in the formation of kidney stones by alleviating endoplasmic reticulum stress and apoptosis of renal tubular epithelial cells. *Redox Report*, **29**(1): 2416825.

Su Y, Li S, Li X, et al. 2024b. Tartronic acid as a potential inhibitor of pathological calcium oxalate crystallization. *Advanced Science*, **11**(21): 2400642.

Sun P, Liao SG, Yang RQ, et al. 2022. *Aspidopterys obcordata* vine inulin fructan affects urolithiasis by modifying calcium oxalate crystallization. *Carbohydrate Polymers*, **294**: 119777.

Sun P, Yue JR, Lu CL, et al. 2024. Targeting urinary calcium oxalate crystallization with inulin-type AOFOS from *Aspidopterys obcordata* hemsl. for the management of rat urolithiasis. *Journal of Ethnopharmacology*, **329**: 118149.

Taguchi K, Chen L, Usawachintachit M, et al. 2020. Fatty acid-binding protein 4 downregulation drives calcification in the development of kidney stone disease. *Kidney International*, **97**(5): 1042–1056.

Tawashi R, Cousineau M, Sharkawi M. 1980. Calcium oxalate crystal formation in the kidneys of rats injected with 4-hydroxy-L-proline. *Urological Research*, **8**(2): 121–127.

Taylor EN, Stampfer MJ, Curhan GC. 2005. Obesity, weight gain, and the risk of kidney stones. *JAMA*, **293**(4): 455–462.

Tenenhouse HS. 2005. Regulation of phosphorus homeostasis by the type IIa Na/phosphate cotransporter. *Annual Review of Nutrition*, **25**: 197–214.

Thiebaut C, Eve L, Poulard C, et al. 2021. Structure, activity, and function of PRMT1. *Life*, **11**(11): 1147.

Thomas J, Thomas E, Balan L, et al. 1971. Experimental oxalic lithiasis induced by hydroxyproline. *Comptes Rendus des Seances de la Societe de Biologie et de Ses Filiales*, **165**(2): 264–267.

Thumchai R, Lulich J, Osborne CA, et al. 1996. Epizootiologic evaluation of urolithiasis in cats: 3, 498 cases (1982–1992). *Journal of the American Veterinary Medical Association*, **208**(4): 547–551.

Tian L, Liu Y, Xu XF, et al. 2022. *Lactiplantibacillus plantarum* J-15 reduced calcium oxalate kidney stones by regulating intestinal microbiota, metabolism, and inflammation in rats. *FASEB Journal*, **36**(6): e22340.

Tokonami N, Takata T, Beyeler J, et al. 2018. Uromodulin is expressed in the distal convoluted tubule, where it is critical for regulation of the sodium chloride cotransporter NCC. *Kidney International*, **94**(4): 701–715.

Trojan BP, Trojan SJ, Navetta A, et al. 2017. Novel porcine model for calcium oxalate stone formation. *International Urology and Nephrology*, **49**(10): 1751–1761.

Tzou DT, Taguchi K, Chi T, et al. 2016. Animal models of urinary stone disease. *International Journal of Surgery*, **36**: 596–606.

Upala S, Jaruvongvanich V, Sanguankeo A. 2016. Risk of nephrolithiasis, hyperoxaluria, and calcium oxalate supersaturation increased after roux-en-y gastric bypass surgery: a systematic review and meta-analysis. *Surgery for Obesity and Related Diseases*, **12**(8): 1513–1521.

Vidgren G, Vainio-Siukola K, Honkasalo S, et al. 2012. Primary hyperoxaluria in coton de tulear. *Animal Genetics*, **43**(3): 356–361.

Viswanathan P, Rimer JD, Kolbach AM, et al. 2011. Calcium oxalate monohydrate aggregation induced by aggregation of desialylated Tamm-Horsfall protein. *Urological Research*, **39**(4): 269–282.

Wakileh GA, Hohmann M, Rassweiler-Seyfried MC, et al. 2024. Visually navigated, ultrasound-guided, freehand percutaneous calyceal puncture - preclinical evaluation of a novel device to simplify a complex surgical task. *Ultrasound International Open*, **10**: a23247668.

Wang CH, Spradling AC. 2020. An abundant quiescent stem cell population in *drosophila* Malpighian tubules protects principal cells from kidney stones. *eLife*, **9**: e54096.

Wang SY, Ju YJ, Gao LJ, et al. 2022. The fruit fly kidney stone models and their application in drug development. *Heliyon*, **8**(4): e09232.

Wang YN, Kreider W, Hunter C, et al. 2018. An in vivo demonstration of efficacy and acute safety of burst wave lithotripsy using a porcine model. *Proceedings of Meetings on Acoustics*, **35**(1): 020009.

Wang Z, Zhang Y, Zhang JW, et al. 2021. Recent advances on the mechanisms of kidney stone formation (review). *International Journal of Molecular Medicine*, **48**(2): 149.

Wei W, Chen M, Xie L, et al. 2024. Comparison of temperature and renal tissue thermal damage by holmium laser with different energy parameters during lithotripsy: in vitro porcine kidney model. *International Urology and Nephrology*, **56**(8): 2539–2545.

Weissbuch I, Leiserowitz L. 2008. Interplay between malaria, crystalline hemozoin formation, and antimalarial drug action and design. *Chemical Reviews*, **108**(11): 4899–4914.

Wesson JA, Ganne V, Beshensky AM, et al. 2005. Regulation by macromolecules of calcium oxalate crystal aggregation in stone formers. *Urological Research*, **33**(3): 206–212.

Wesson JA, Johnson RJ, Mazzali M, et al. 2003. Osteopontin is a critical inhibitor of calcium oxalate crystal formation and retention in renal tubules. *Journal of the American Society of Nephrology*, **14**(1): 139–147.

Wesson JA, Zenka R, Lulich J, et al. 2022. Comparison of cat and human calcium oxalate monohydrate kidney stone matrix proteomes. *Urolithiasis*, **50**(6): 653–664.

Wesson JA, Zenka R, Sherman K, et al. 2024. Comparison of cat stone matrix and cat urine proteomes to human calcium oxalate stone matrix and urine proteomes. *Urolithiasis*, **52**(1): 130.

Worcester EM. 1996. Inhibitors of stone formation. *Seminars in Nephrology*, **16**(5): 474–486.

Worcester EM, Coe FL. 2010. Clinical practice. Calcium kidney stones. *The New England Journal of Medicine*, **363**(10): 954–963.

Wu F, Cheng YY, Zhou JF, et al. 2023. Zn^{2+} regulates human oxalate metabolism by manipulating oxalate decarboxylase to treat calcium oxalate stones. *International Journal of Biological Macromolecules*, **234**: 123320.

Wu ML, He C, Yu H, et al. 2025. Therapeutic targets of antidiabetic drugs and kidney stones: a druggable mendelian randomization study and experimental study in rats. *European Journal of Pharmacology*, **987**: 177197.

Xu YX, Liang H, Xia KG, et al. 2025. Umbelliferone attenuates calcium oxalate crystal-induced renal injury and inflammation by attenuating autophagy through the PI3K/AKT pathway. *International Immunopharmacology*, **150**: 114250.

Yamaguchi S, Wiessner JH, Hasegawa AT, et al. 2005. Study of a rat model for calcium oxalate crystal formation without severe renal damage in selected conditions. *International Journal of Urology*, **12**(3): 290–298.

Yamashita S, Komori T, Kohjimoto Y, et al. 2020. Essential roles of oncostatin M receptor β signaling in renal crystal formation in mice. *Scientific Reports*, **10**(1): 17150.

Yang H, Male M, Li Y, et al. 2018. Efficacy of hydroxy-L-proline (HYP) analogs in the treatment of primary hyperoxaluria in *Drosophila melanogaster*. *BMC Nephrology*, **19**(1): 167.

Yang JH, Li ZH, Lai C, et al. 2024. An in vivo assessment of a novel temperature control flexible ureteroscope system for monitoring and controlling intrarenal temperature during flexible ureteroscopy. *Urology*, **191**: 38–44.

Yang Y, Dou XD, Sun YZ, et al. 2025. Enhancer profiling reveals a protective role of RXRα against calcium oxalate-induced crystal deposition and kidney injury. *Advanced Science*, **12**(21): 2411735.

Ye C, Jiang W, Hu T, et al. 2024. The regulatory impact of CFLAR methylation modification on liver lipid metabolism. *International Journal of Molecular Sciences*, **25**(14): 7897.

Ye T, Yang XQ, Liu HR, et al. 2021. Theaflavin protects against oxalate calcium-induced kidney oxidative stress injury via upregulation of SIRT1. *International Journal of Biological Sciences*, **17**(4): 1050–1060.

Yuan TH, Xia YQ, Li BJ, et al. 2023. Gut microbiota in patients with kidney stones: a systematic review and meta-analysis. *BMC Microbiology*, **23**(1): 143.

Yuan TH, Ye ZH, Mei SQ, et al. 2025. PRMT1-mediated methylation of UBE2m promoting calcium oxalate crystal-induced kidney injury by inhibiting fatty acid metabolism. *Cell Death & Disease*, **16**(1): 579.

Zeng GH, Mai ZL, Xia SJ, et al. 2017. Prevalence of kidney stones in China: an ultrasonography based cross-sectional study. *BJU International*, **120**(1): 109–116.

Zhang HY, Yang HX, Du S, et al. 2025. Rutin ameliorates calcium oxalate crystal-induced kidney injury through anti-oxidative stress and modulation of intestinal flora. *Urolithiasis*, **53**(1): 50.

Zhang XZ, Lei XX, Jiang YL, et al. 2023. Application of metabolomics in urolithiasis: the discovery and usage of succinate. *Signal Transduction and Targeted Therapy*, **8**(1): 41.

Zhou DH, Wu Y, Yan H, et al. 2022. Gallic acid ameliorates calcium oxalate crystal-induced renal injury *via* upregulation of Nrf2/HO-1 in the mouse model of stone formation. *Phytomedicine* , **106**: 154429.

Zhu Q, Wang DH, Liang F, et al. 2022. Protein arginine methyltransferase PRMT1 promotes adipogenesis by modulating transcription factors C/EBPβ and PPARγ. *Journal of Biological Chemistry*, **298**(9): 102309.

Zhu W, Zhao ZJ, Chou FJ, et al. 2019. Loss of the androgen receptor suppresses intrarenal calcium oxalate crystals deposition via altering macrophage recruitment/M2 polarization with change of the miR-185-5p/CSF-1 signals. *Cell Death & Disease*, **10**(4): 275.